From seascape ecology to population genomics and back. Spatial and ecological differentiation among cryptic species of the red algae Lithophyllum stictiforme/L. cabiochiae, main bioconstructors of coralligenous habitats

Aurelien de Jode, Romain David, Anne Haguenauer, Abigail Cahill, Zinovia Erga, Dorian Guillemain, Stéphane Sartoretto, Caroline Rocher, Marjorie Selva, Line Le Gall, et al.

Molecular Phylogenetics and Evolution (2019) 137: 104-113
doi: 10.1016/j.ympev.2019.04.005

From seascape ecology to population genomics and back. Spatial and ecological differentiation among cryptic species of the red algae *Lithophyllum stictiforme/L. cabiochiae*, main bioconstructors of coralligenous habitats

Aurélien De Jode[a,*], Romain David[a], Anne Haguenauer[a,b], Abigail E. Cahill[a,c], Zinovia Erga[a], Dorian Guillemain[a,d], Stéphane Sartoretto[e], Caroline Rocher[a], Marjorie Selva[a], Line Le Gall[f], Jean-Pierre Féral[a], Anne Chenuil[a]

[a] *Aix Marseille Univ, Univ Avignon, CNRS, IRD, IMBE, Marseille, France*
[b] *EPHE PSL Research University, USR 3278 CRIOBE CNRS-UPVD, BP 1013, Moorea 98729, French Polynesia*
[c] *Biology Department, Albion College, MI 49224, USA*
[d] *Institut Pythéas: Observatoire des Sciences de l'Univers, France*
[e] *IFREMER, Zone Portuaire de Brégaillon, 83500 La Seyne-sur-mer, France*
[f] *Institut Systématique Evolution Biodiversité (ISYEB), Muséum national d'Histoire naturelle, CNRS, Sorbonne Université, EPHE, Université des Antilles, 57 rue Cuvier, CP 39, 75005 Paris, France*

A B S T R A C T

Ecosystem engineering species alter the physical structure of their environment and can create or modify ha-bitats, having a massive impact on local biodiversity. Coralligenous reefs are highly diverse habitats endemic to the Mediterranean Sea built by calcareous benthic organisms among which Crustose Coralline Algae are the main engineering species. We analyzed the diversity of *Lithophyllum stictiforme* or *L. cabiochiae* in coralligenous habitats combining a multiple barcode and a population genomics approach with seascape features. Population genomics allowed disentangling pure spatial effects from environmental effects. We found that these taxa form a complex of eight highly divergent cryptic species that are easily identifiable using classic barcode markers (*psb*A, LSU, COI). Three factors have a significant effect on the relative abundances of these cryptic species: the location along the French Mediterranean coast, depth and Photosynthetic Active Radiation (PAR). The analysis of around 5000 SNPs for the most abundant species revealed genetic differentiation among localities in the Bay of Marseille but no differentiation between depths within locality. Thus, the effect of depth and PAR on cryptic species communities is not a consequence of restricted connectivity but rather due to differential settlement or survival among cryptic species. This differential is more likely driven by irradiance levels rather than by pressure or temperature. Both the genetic and species diversity patterns are congruent with the main patterns of currents in the Bay. Ecological differentiation among these engineering cryptic species, sensitive to ocean warming and acidification, could have important consequences on the diversity and structure of the coralligenous commu-nities.

Keywords:
Engineering species
Cryptic species
Ecological niche
Coralligenous habitats
Ecological differentiation
Crustose Coralline Algae

1. Introduction

Ecosystem engineers are organisms that alter their abiotic environment in such a way that they create or modify habitats, thereby having large effects on the associated species community (Jones et al., 1994; Crain & Bertness, 2006). Thus, phenotypic variation among ecosystem engineering organisms potentially have important consequences on the species community and on the ecosystem (Whitham et al., 2003). The phenotypic variation can arise at the intra specific level by plasticity or genetic differentiation, as well as interspecifically when different engineering species have different ecological traits (Badano & Cavieres, 2006; Lamit et al., 2011). In the marine realm, animal organisms acting as ecosystem engineers promote biodiversity of the associated communities (Romero et al., 2015). Algal

engineer species also have tremendous impacts on marine biodiversity. Within seascapes, kelp forests are the most conspicuous three-dimensional habitats hosting a high diversity of species (Teagle et al., 2017). Crustose Coralline Algae (hereafter CCA) are also major engineering organisms and contribute to the three-dimensional structure of several habitats such as coral reefs, maërl beds and coralligenous habitats.

In the Mediterranean Sea, coralligenous habitats are emblematic calcareous biogenic constructions built-up in dim light conditions mainly by calcareous algae (Corallinacea and Peyssonneliacea) and reinforced by calcareous invertebrates (e.g. bryozoans, serpulid polychaetes, scleractinians) (Ballesteros, 2006). The resulting framework is complex and harbors various micro-habitats that shelter at least 1600 species (Ballesteros, 2006), making coralligenous habitats an important biodiversity hot-spot in the Mediterranean Sea (Boudouresque, 2004). These habitats provide various ecosystem services (e.g. food provisioning, recreational diving, research material) (Paoli et al., 2016; Thierry de Ville 'Avray et al., 2019), yet they are threatened by global ocean warming and acidification (Martin & Gattuso, 2009; Lombardi et al., 2011; Martin et al., 2013; Linares et al., 2015; Rodríguez-Prieto, 2016) and local human activities (e.g. fishing, anchoring or sewage outfalls) (Hong, 1980; Ballesteros, 2006; Balata et al., 2005; Balata et al., 2007). The lack of knowledge regarding the biodiversity of these habitats impedes our understanding of their ecological functioning and our capacity to protect them efficiently (SPA/RAC, 2017).

In coralligenous habitats, CCA are considered to be the major engineering group (Laborel, 1961; Laubier, 1966; Sartoretto et al., 1996); however, the phylogenetic affinities of these CCA among other Corallinales has not been tested yet with molecular systematic tools even though these tools have strongly modified the perception of coralline diversity (Bittner et al., 2011; Pardo et al., 2014; Peña et al., 2015; Rösler et al., 2016). In the genus *Lithophyllum*, *L. stictiforme* (Areschoug) Hauck (1877) *and L. cabiochiae* (Boudouresque & Verlaque) Athanasiadis (1999) are considered the main coralligenous builders below 20 m depth (Sartoretto et al., 1996). However, identification of these two nominal species based on macro-morphological character-istics or anatomical structures is uncertain. Moreover, recent studies using molecular systematic tools (Rindi et al., 2017; Pezzolesi et al., 2019) have revealed the presence of cryptic diversity but did not sup-port distinction between these two species.

Ignoring the presence of cryptic species within a nominal species may have important consequences for biodiversity management. In particular, when cryptic species are ecologically differentiated, environmental changes may result in higher risks of extinction (local or global) than expected for a single generalist species (Chenuil et al., in press). Furthermore, recent studies showed that *"L. stictiforme"* survival and reproduction were affected by irradiance levels and temperature (Rodríguez-Prieto, 2016) and that *"L. cabiochiae"* photosynthesis was reduced under elevated pCO_2 (Martin et al., 2013). This highlights the need for studies of biodiversity at both inter- and intraspecific levels to evaluate the potential of adaptation to global change of these ecosystem engineering species.

In this study, we combined barcoding and exon capture sequencing to reveal cryptic species among 438 individuals initially collected as *L. cabiochiae/stictiforme* found in sympatry along the French Mediterranean coast, providing the opportunity to study the ecological determinants of their co-distribution. We used a fine scale, ecologically contextualized design in order to distinguish spatial effects (resulting from migration and connectivity) from ecological effects (fitness dif-ferences among cryptic species in distinct environments). Light is the most important environmental factor shaping coralligenous commu-nities (Ballesteros, 2006), thus we recorded environmental variables affecting the irradiance levels received by the community on each site. We analyzed community composition within the species complex (i.e. the relative abundances of the distinct cryptic species) in relation to ecological conditions (location, depth, orientation, slope) to determine if the different species were found in different niches. Population genetic analyses were then carried out in the most abundant of the cryptic species to determine the connectivity matrix among studied locations in order to disentangle pure spatial effects from environmental effects of depth.

2. Materials and methods

2.1. Field sampling and DNA extraction

Samples were collected by scuba diving in 13 different localities along the continental French Mediterranean coast and in Corsica (Figs. 2 & 3, Supplementary Material I). In the Marseille and Toulon area, horizontal transect lines were divided into 5 m segments. For each segment, up to 4 fragments of *Lithophyllum* spp. of about 3 cm large were collected. To avoid sampling clones of the same specimen, we left a minimum of 1 m between collected specimens. An average of 16 samples was collected at each sampling site. Moreover, 3 physical parameters were recorded in situ: slope, orientation, and rugosity. Slope was divided into 4 levels: (i) "Flat", when the angle formed by the substrate with the horizontal line was between 0° and 18.45°, (ii) "In-clined", for angles between 18.45° and 71.69°, (iii) "Vertical", for angles between 71.69° and 90° and (iv) overhanging, when there is an over-hang at least as large as a person above the observer and covers most of the segment. Orientation was measured with a compass handled by the diver and directed perpendicularly to the substrate wall (in the hor-izontal plane; it could not be defined for horizontal slopes). We con-sidered 8 modalities: North (N), South (S), East (E), West (W) and the four intermediate orientations (Northeast (NE), Northwest (NW), Southeast (SE), Southwest (SW)). Note that a North orientation in our dataset corresponds to a South exposition of the substrate. Rugosity characterizes the size of crevices, holes and faults observed in the segment and was characterized as follows: (i) "Tiny", when holes were smaller than a fist (about 10 cm wide); (ii) "Small", when holes were larger than a fist but smaller than a head; (iii) "Medium" (M): holes and crevices that were approximately head-sized (about 30 cm wide); (iv) "Large" (L): crevices, holes and faults can contain at least the upper body (about 1 m wide with air tanks). Most transects were carried out at a depth of 24–31 m (depth category D1), or 37–46 m (depth category D2). In Banyuls-sur-mer, Villefranche-sur-mer and Corsica transects were not segmented and all individuals were sampled at the same depth category. All CCA were dried, and preserved in silica gel at room temperature in a dark place or in ethanol 96% at 4 °C until DNA ex-traction. A piece of algal tissue was excised and cleaned of epiphytes by scraping the surface with a razor blade. The excised sample was dis-rupted using a TissueLyser II system (Qiagen) with a 3 mm stainless steel bead. DNA was extracted using Chelex 100 chelating resin (Walsh et al., 1991). Around 20 mg of tissue along with 500 μL of Chelex 10%and 3 μL of Proteinase K (20 mg/mL) were incubated at 60 °C for 90 min. Then sample was heated at 100 °C for about 10 min to deacti-vate the Proteinase K.

2.2. Sanger sequencing

Three independent molecular markers were used to identify the species of *Lithophyllum*: the plastid marker *psb*A, (primers psbA-F and psbA-R2, Yoon et al., 2002), a fragment of the nuclear 28S (or large subunit) rDNA marker (primers T04 and T15, Harper & Saunders, 2001) and the mitochondrial marker COI (primers GazF1 and GazR1, Saunders, 2005). PCR reaction mixes were the same for the three markers, and PCR programs were identical for *psb*A and 28S (Supplementary Material II). PCR products were verified by electrophoresis migration on 1.5% agarose gel TBEx1 and then sent to Eurofins Genomics for Sanger sequencing using primers Gaz-R1, *psb*A-F and T04. Fragment sizes were approximately 700 bp for COI and 1000 bp for *psb*A and 28S. Sequences were checked and aligned using BioEdit software (Hall, 1999) before further analyses.

2.3. Miseq sequencing

In a second step, to determine the lineages of additional individuals with lower sequencing costs, we designed shorter fragments within the *psb*A and 28S markers to allow high throughput sequencing (Illumina, Miseq paired end 2 × 250 bp) (Supplementary Material II). PCR cycles and reactions mixes were the same for both markers (Supplementary Material II). Amplicons were sequenced, and Miseq Reads were processed as described in Cahill et al., (2017) with a few exceptions. For the plastid marker, *psb*A, sorting was done as in Cahill et al. (2017) for mitochondrial loci with slight modifications: sequences were retained if the total number of reads was ≥20 (i.e. 20× coverage) and the count ratio ≤0.14 (i.e. the most abundant read was at least 7 times more abundant than the second most abundant read). For the 28S nuclear locus, the total number of reads was sufficient for all individuals (at least 66 reads for each). For both markers, forward and reverse reads did not overlap and were attached end to end.

2.4. Haplotype networks

For each marker, sequences from Sanger sequencing and Miseq sequencing were aligned visually with Bioedit (Hall, 1999). Sequence positions found in both Sanger and Miseq sequencing were kept to build an alignment with all sequences of the same size. For each marker, we built haplotype networks from the longer sequence alignment obtained by Sanger sequencing and also, for *psb*A and 28S, from the shorter alignments including Miseq sequences. Haplotype networks were generated using the median-joining algorithm of the Network software, v.5.0.0.1 (Bandelt et al., 1999). The average proportion of differences and average Kimura distance (K2P, Kimura, 1980) between haplogroups were computed from the long alignments (i.e. using MEGA v.4 (Tamura et al., 2007)).

2.5. Transcriptomics

Individuals were collected in 2015 at the CAS, MEJ, LPD, COU localities by scuba diving, and preserved in seawater during transportation to the lab. Around 2 cm^2 of each individual was immediately cleaned of epiphytes with a razor blade, placed in 1 ml QIAzol lysis reagent (Qiagen) and disrupted using TissueLyserII instrument (Qiagen). The rest was preserved in 96% ethanol at 4 °C and used to determine the haplogroup of each individual following the protocol for Sanger sequencing described above in this paper.

Total RNA isolation was performed according to the manufacturer's instructions, except for overnight precipitation at −20 °C (1/10 vol sodium acetate 3 M pH 5.2, 2 volumes ethanol). Contaminants were eliminated by further cleaning using an RNeasy plus mini kit (Qiagen). RNA integrity was assessed using Agilent 2100 *Bioanalyzer* system, and concentration and purity using Nanodrop instrument (Thermofisher). Residual DNA was digested using TurboDNAse (Ambion) following the manufacturer's instructions.

RNA-Seq libraries were generated using the TruSeq Stranded mRNA Illumina kit according to the manufacturer's protocol. During this preparation, libraries were individually tagged to allow their pooling before sequencing. The size distributions of libraries' RNA fragments were controlled with a Fragment Analyzer™ Automated CE System from Advanced Analytical Technologies, Inc. (AATI).

The eight libraries were quantified by qPCR following the manufacturer's protocol. Libraries were pooled before sequencing on one lane on the Illumina HiSeq3000 (Illumina Inc., San Diego, CA) as paired-end reads of length 150 bp. Library preparation and sequencing were performed at the Genotoul platform (http://get.genotoul.fr/).

Three samples were highly contaminated with 30%, 10% and 7% of their reads mapping against the *E. coli* genome. Those reads were removed before the assembly step. Assembly of each library was performed using the RunDrap Pipeline with default parameters as described by Cabau et al. (2017).

To build a reference transcriptome, one meta-assembly of the two individuals of the most abundant species (the C1 species) transcriptome was conducted, using the Run Meta Pipeline described in Cabau et al. (2017).

Sequences from each assembly and meta-assembly were blasted using the program blastn version 2.2.26 (Altschul et al., 1990; Camacho et al., 2009) against different databases available on the Genotoul Cluster: Bacteria (ftp://ftp.ncbi.nih.gov/genomes/archive/old_refseq/Bacteria), H_sapiens (ftp://ftp.ncbi.nih.gov/genomes/H_sapiens), Drosophila_melanogaster (ftp://ftp.ncbi.nih.gov/genomes/archive/old_refseq/Drosophila_melanogaster), yeast (ftp://ftp.ncbi.nih.gov/blast/db/FASTA/) , M_musculus (ftp://ftp.ncbi.nih.gov/genomes/M_musculus) and contigs with a hit (e-value threshold 0.001) against any of them were removed from further analyses. These species are commonly used in genomic studies and are potential sources of contamination on the genomic platform. Also, their genomes are available allowing to compare our sequences with these potential contaminants.

The meta-assembly of the two individuals of the C1 haplogroup was used as a reference in the following steps and contig names were modified using a custom script. For all individuals, reverse reads were renamed and pooled with forward reads in one file. All reads were mapped on the reference with Bwa mem (Li, 2013) with default parameters. SNP calling was conducted using the Reads2snp v2.0 script from PopPhyl project (Tsagkogeorga et al., 2012; Gayral et al., 2013). Open reading frames (ORFs) were detected using Transdecoder 3.0.0 (Haas, 2013) and the ORF output file was converted to get.ORF format using a custom script.

Biotinylated RNA probes were designed by and ordered from MYcroarray (Ann Arbor, MI, USA; now Arbor Biosciences). Based on the ORF sequences, 18757 candidate sequences (total size 18.3 Mb) were soft-masked for simple repeats and low-complexity DNA using RepeatMasker (Smit et al., 2013). Any strings of Ns between 1 and 10 bp were replaced with Ts to facilitate probe design; larger strings of Ns were left alone. 120 bp probes with 2× flexible tiling density were designed for all sequences, and dG, GC%, and % soft-masked were ta-bulated. Only probes with (i) dG greater than −9, (ii) 30–50% GC, (iii) 0 soft-masked bases were kept and divided in two subsets: the first one contained probes with 1 to 7 SNPs with the reference and the second one the probes with no SNP with the reference.

Among the first probe subset we randomly sampled one probe per ORF for a total of 14403 probes. For each randomly selected probe we extracted the closest and the furthest probe when possible. Finally, we took 2000 probes in the closest, 2000 in the furthest (from the first probe selected in the ORF) and 1617 in the non-polymorphic probes for a total of 20020 probes.

2.6. Exon-Capture genotyping

For capture sequencing, total genomic DNA was extracted according a protocol derived from Sambrook et al. (1989), followed by one or two purifications using NucleoSpin® gDNA Clean-up (Macherey-Nagel) (see Supplementary Material III for a detailed protocol).

DNA was fragmented using The Bioruptor® Pico (diagenode) to obtain fragment size of around 250 pb. Dual-indexed NGS Libraries were made using NEBNext® Ultra™ DNA Library Prep Kit for Illumina® kit following the manufacturer's protocol. Two conditions of in-solution target enrichment were performed according to manufacturer's recommendations following the MYbaits v3 protocol (http://www.mycroarray.com/mybaits/manuals.html).

The first condition was 32 libraries in 30 μL reactional volume, repeated 3 times for a total of 128 enriched libraries, whereas the second condition was conducted in 15 μL reactional volume with 16 libraries. Post-capture, libraries were amplified following Mybaits protocol recommendations (Mix KAPA HiFi, PCR at 60 °C, 14 cycles), post PCR purification using Ampure XP, and 1.6 pM DNA was provided for

sequencing on one MID flowcell of NextSeq Illumina System, Paired-end sequencing (2 × 150bp).

First, raw reads were split according to their sequencing lane using a custom python script and fastq files were converted to SAM files. We followed the GATK good practices (Van der Auwera et al., 2013) to call SNPs except for the BQSR and VQSR steps because of the lack of reference SNPs data sets. We used ORFs of the C1 haplogroup meta assembly as a reference in all the above steps and SNPs calling was restricted to an area starting 400 bp before the first base covered by the probe to 400 bp after the last base covered by the probe.

To study the inter haplogroup divergence the jointGenotyping step was conducted with all individuals from the Bay of Marseilles. To study the intra C1 haplogroup diversity the jointGenotyping step was conducted with all individuals from the C1 haplogroup. In both cases, obtained SNPs were filtered based on GATK recommended parameters (QD < 2.0, FS > 60.0, MQ < 40.0, MQRankSum < -12.5, ReadPosRankSum < -8.0), then SNPs with minor allele frequency lower than 0.01 were removed. For the inter haplogroup study, SNPs with more than 10% missing value were removed from the dataset. For the intra C1 haplogroup dataset, SNPs with more than 25% missing values or failing HWE in one or more of the 7 populations were re-moved using vcftools (Danecek et al., 2011), with a p-value threshold of 0.01. Finally, for both datasets one SNP per ORF was randomly ex-tracted using a custom python script and individuals with more than 20% missing genotypes were excluded from the dataset.

2.7. Population genomics analyses

First, a neighbor joining tree on multilocus genotypes was built with individuals of the inter clade dataset using the APE package (Paradis et al., 2004) i n R (R Core team, 2017). Individuals were colored according to their haplogroup determined by one of the three barcoding markers. Individuals with undetermined haplogroups were assigned to a species based on their positions in the tree, using the phytools (Revell, 2012) package in R (R Core team, 2017). Principal Component analyses (PCA) were conducted on individuals assigned to the C1 species using the adegenet R package (Jombart, 2008; Jombart & Ahmed, 2011). Calculation of F statistics, diversity indices, and tests of genetic differentiation were carried out with the GENEPOP R package (Rousset, 2008).

2.8. Clonality

To assess the importance of clonal reproduction in the C1 species we used the functions genet_dist and genet_dist_sim from the Rclone package (Bailleul et al., 2016). The genet_dist function was used to compute a matrix of pairwise number of alleles differences between our multilocus genotypes (MLG) in each population. The genet_dist_sim function allowed for simulation of a sexual reproduction event between pairs of unique MLGs (outcrossing) or pairs of MLGs (partial selfing) of all our populations and computed two matrices of pairwise genetic distances within the resulting population after 1000 sexual events (one generation each). The first matrix was obtained by simulating sexual reproduction including outcrossing and selfing and the second was obtained by simulating only outcrossing events (no selfing). The three distributions (empirical, simulated with selfing and simulated without selfing) were compared to assess if the distribution of empirical distances can be obtained by sexual reproduction alone. We performed the analysis on 2176 biallelic SNPs without missing values.

2.9. Community analyses

All the community statistical analyses were conducted using the PRIMER software version7 (Clarke et al., 2014 & 2015). Due to the different sampling procedure, the Banyuls-sur-mer, Villefranche-sur-mer and Corsica localities were not used in statistical analyses linking community composition to environmental factors (PERMANOVAs and PERMANCOVAs). However, all the localities were used in the non-metric Multi-Dimensional Scaling (nMDS) and for the estimation of diversity indices. The final community matrix used for the Marseille area contained 187 rows, corresponding to each segment of marine substrate, and for each row, the number of individuals of each of the 7 species present in this area (corresponding to 7 columns). The final environmental matrix had the same row number and names as the final community matrix, and for each row, the level of each of the environmental variables (depth category, locality, orientation, slope, rugosity). Community data were standardized by the total number of individuals and square-root transformed before computing pairwise Bray-Curtis dissimilarity indices. To calculate diversity metrics for each locality, we summed the abundances of each segment (Table 1). The nMDS was produced using Bray-Curtis similarity indices on the table of abundances per locality.

Table 1
Community diversity index for each locality. S: total number of species. N: total number of individuals. D: Margalef species richness index. J': Pielou evenness index. H': Shannon index,1-Lambda': Simpson corrected for small samples. N1: Hill number of order one. N2: Hill number of order 2.

Locality	S	N	D	J'	H'	1-LAMBDA'	N1	N2
BPT	3	25	0.6213	0.835	0.9174	0.57	2.503	2.208
CAS	5	67	0.9513	0.7326	1.179	0.592	3.252	2.399
CIR	5	69	0.9447	0.3603	0.5799	0.2835	1.786	1.388
COU	2	19	0.3396	0.9495	0.6581	0.4912	1.931	1.87
CSC	3	28	0.6002	0.6908	0.7589	0.455	2.136	1.782
CTF	2	37	0.2769	0.909	0.6301	0.4505	1.878	1.78
FTF	3	51	0.5087	0.2904	0.319	0.1498	1.376	1.172
LDM	3	34	0.5672	0.4039	0.4438	0.221	1.559	1.273
LPD	3	20	0.6676	0.865	0.9503	0.5895	2.586	2.273
MEJ	3	58	0.4926	0.6568	0.7216	0.4168	2.058	1.694
MOY	3	56	0.4969	0.3145	0.3456	0.1682	1.413	1.198
PLN	2	28	0.3001	0.8113	0.5623	0.3889	1.755	1.6
VPR	4	15	1.108	0.9665	1.34	0.781	3.818	3.689

Due to the lack of replication, the PERMANOVA designs only included 2 factors: locality as a random factor, one other environmental factor as a fixed factor and the interaction term between the two. The PERMANCOVAs designs included the locality factor and the depth (as a numeric variable) or the Photosynthetic Active Radiation (PAR) as covariable. The PAR was calculated for each depth by averaging the values obtained from the SOMLIT recorder in the Frioul locality between 2007 and 2017. Thus, PAR was not directly measured at each location but, according to its depth, each sampling segment was assigned an estimated PAR value. Since the effect of the 'location' factor was considered in the analysis using the PAR covariable, the variable PAR represents the effect that depth has on irradiance attenuation.

3. Results

3.1. Haplotype networks

Sanger (i.e. longer) sequence alignments were respectively 594 bp, 744 bp and 802 bp for the mitochondrial (COI), plastid (*psb*A) and the nuclear markers (28S rDNA), after primers and lower quality terminal regions were removed. Shorter alignments including Miseq sequences for the *psb*A and 28S markers were respectively 365 bp and 425 bp. Figures in Supplementary Material IV display the networks built from subsets of individuals which had been sequenced for several markers (Fig. networks: 3 sanger, 2 Miseq). Seven haplogroups were identified in the haplotype network built from long *psb*A sequences: C1, C2, C3, C4, C5, C6 and C7. The individual compositions of these seven hap-logroups perfectly matched with those of seven haplogroups formed by the other markers (with the exception of a single individual, likely a contamination or a labeling error), for both long and short alignments

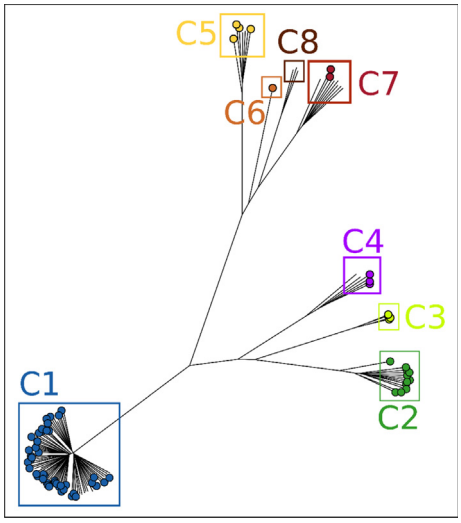

Fig. 1. Neighbour Joinning tree based on euclidean distances between individual multiloci genoptype obtained by capture sequencing (7068 SNPs). Individuals are colored according to their haplogroup determined using the psbA marker. Uncolored tips correspond to individuals with no barcoding sequence.

(273 individuals were sequenced for both the 28S rDNA and *psb*A markers). The number of substitutions separating the distinct haplogroups varied (in long alignments) from 4 to 22 for the most conserved marker which is the 28S rDNA, from 14 to 48 for *psb*A and from 40 to 77 for COI, the most rapidly evolving marker (Supplementary Material IV). The minimum and maximum Kimura distances were respectively 0.003 (28S rDNA, C6-C7) and 0.105 (COI, C1-C6) (Supplementary Material IV). Since the haplogroups were congruent among markers and found in sympatry, their genetic isolation and their status of cryptic species was established (cf discussion) so in the following sections, they were considered as such.

3.2. Capture sequencing

For the inter species dataset, a total of 7068 SNPs were obtained for 122 individuals. Among these individuals, 69 were already classified in one of the 7 species using at least one of the three barcode markers. For all individuals from the Marseille area, species determination based on barcode marker or the multilocus genotype distances between individuals (in number of different alleles) gave the same results (Fig. 1). Among the 53 remaining individuals, 3 clustered together forming the C8 species, and the others were assigned to one of the 7 species according to their position on the neighbor joining tree. The mean Euclidean distances based on genotypes between individuals of the different species ranged from 52.76 between C7 and C8 to 115.42 between C2 and C5 (Supplementary Material VI). The C4 species had the highest intra species mean distances: 24.10. Three clusters were distinguished on the tree: C1, C2 to C4, and all the C5 to C8 species (Fig. 1).

3.3. Population genomics for the C1 species

For the individuals of the C1 species, a total of 4744 SNPs were obtained for 75 individuals. The expected heterozygosity by population ranged from 0.1090 in FTF_D1 to 0.1603 in RMO. Significant F_{IS} values were found in 4 populations: FTF_D1, FTF_D2, CAS_D1, CAS_D2 ranging from −0.0096 in CAS_D2 to 0.1260 FTF_D1. The global F_{ST} value was 0.0464 and F_{ST} values between pairs of populations ranged from 0.0077 between CAS_D1 and CAS_D2 to 0.0911 between RMO and LPD. The genetic differentiation for the two pairs displaying contrasted depths was not significant. On the PCA plot (Fig. 4), the individuals were clustered according to their localities (but the PCA did not suggest clonality because all individuals were separated on at least one combination of axes). Individuals were spread in three different clusters from left to right on the first axis (5.71% of the total variability). The second axis represented 3.06% of the total variability and no clear cluster was formed along this axis. The third axis represented 2.67% of variability and separated LPD population from all the others (Fig. 4B). In clonality analyses, all multilocus genotypes (MLG) were clearly dis-tinct and empirical genetic distances distributions match with simu-lated genetic distance distributions obtained under the hypothesis of outcrossing in all populations (Supplementary Material VIII).

3.4. Cryptic species diversity and distribution

The species richness among localities ranged from 2 in the COU, CTF and PLN localities to 5 in the CIR and CAS localities. Simpson di-versity indices in localities ranged from 0.1498 at the FTF locality to 0.781 at the VPR locality (Table 1). *Lithophyllum* cryptic species com-munities were differentiated between localities at different spatial scales (Figs. 2, 3 & Table 2 & 3). At large spatial scale, the BPT locality was very distant from all other localities (Fig. 2B) and was the only one where species C1 was absent and where species C5 was present. Then, the VPR locality was isolated from localities of the Marseille area on the nMDS (Fig. 2B) and harbored a high proportion of the C6 and C7 cryptic species as well as the highest species diversity (Table 1). The Corsica community was grouped with communities of the Marseille area (Fig. 2B). At small spatial scale (from the COU locality to the LPD lo-cality), species were not randomly distributed across localities (2 fac-tors PERMANOVA, p(perm) = 0.0001, Table 2 & Fig. 3): the C1 species was ubiquitous and the C2 species was missing in a single locality (COU). Species C5, C7 and C8 were only found in the CAS locality and the C6 species only in the RMO locality. The C4 species was mainly

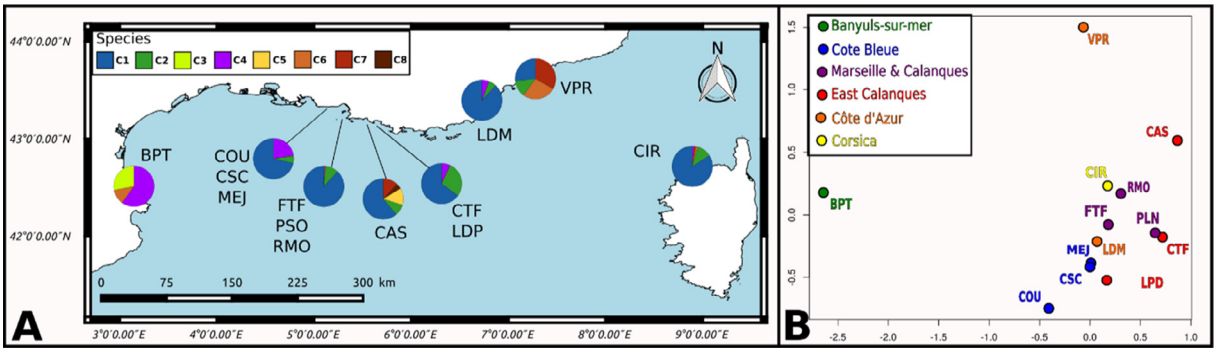

Fig. 2. Distribution of the eight cryptic species along the French Mediterranean coastline. A: Map of the study area with pie chart representing the relative abundances of the cryptic species at the different localities. B: nMDS on Bray-Curtis distances between localities at large spatial scale: from Banyuls-sur-mer to Villefranche-sur-mer and including Corsica. Stress: 0.04.

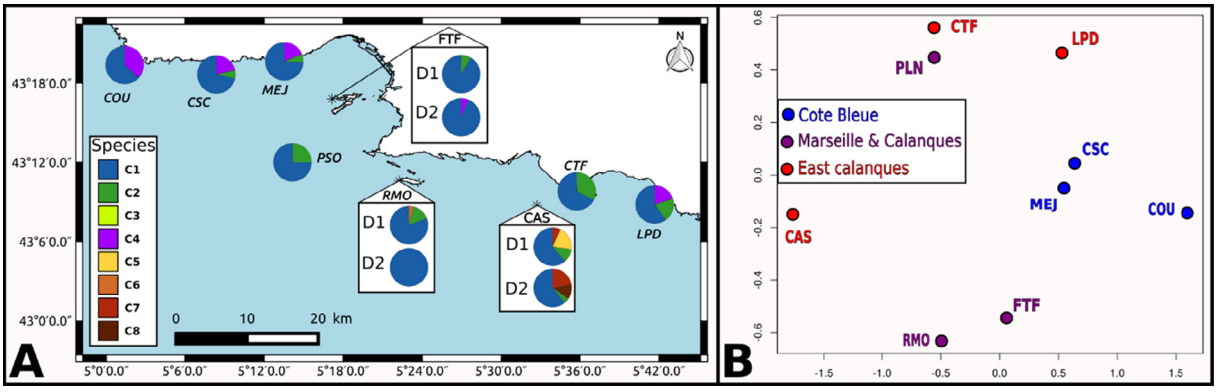

Fig. 3. Distribution of the eight cryptic species around Marseille coastline. A: Map of the Marseille area with pie chart representing the relative abundances of the cryptic species at the different localities and different depth. D1: shallow depth category between 24 and 31 m depth. D2: depth category between 37–46 m. B: nMDS on Bray-Curtis distances between localities at small spatial scale: from the COU locality to the LPD locality. Stress: 0.04.

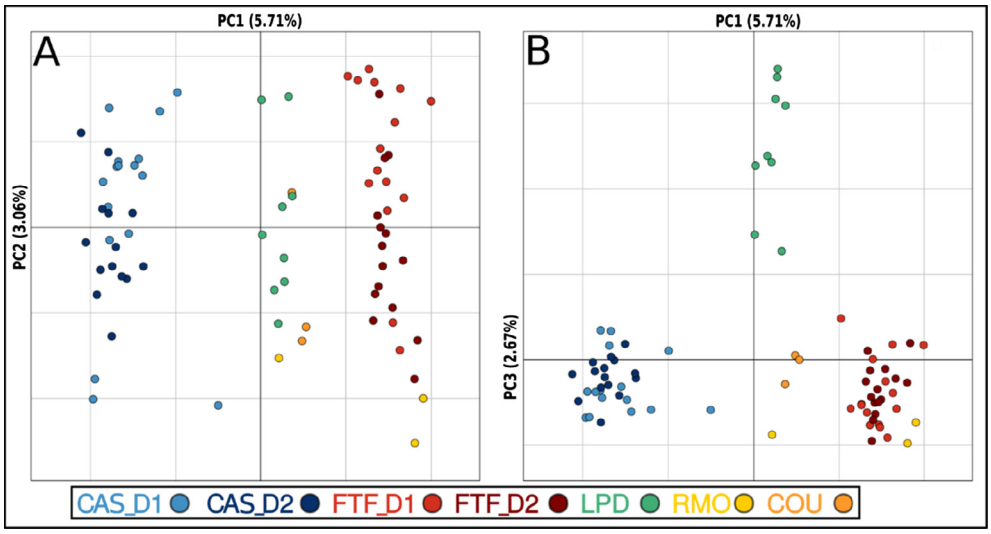

Fig. 4. Principal Component Analysis (PCA) on the multilocus genotype for individuals of the C1 cryptic species. Individuals are colored according to their population, and D1 and D2 in population names correspond to depth categories. A: first and second axes are drawn. B: first and third axes are drawn.

found at the Côte Bleue (COU, MEJ, CSC) with few exceptions (Fig. 3A). Based on the species relative abundances and the nMDS four groups of localities were discernible (Fig. 3): (i) the Côte Bleue (COU, CSC, MEJ) and LPD, (ii) Marseille (FTF, RMO), (iii) the PSO and CTF localities and (iv) the CAS locality was highly distant from all the others.

3.5. *Cryptic species ecology*

In the two-way PERMANOVAs, the random locality factor was always significant, but the fixed environmental factor was never significant (Table 2). However, the interaction between locality and sampling depth category had a significant effect on the *Lithophyllum* cryptic species community composition (PERMANOVA, p (perm) = 0.014). The community differed between the two depth ca-tegories in the RMO locality (PERMANOVA, p(mc) = 0.0439) and the CAS locality (PERMANOVA, p(perm) = 0.0067). In the RMO locality the C2 and C6 species were found at depth 28 m and the most abundant C1 species was found at all depths. In the CAS locality, the C5 species was only found in the D1 depth category, the C8 species was only found in the D2 depth category (Fig. 3A). In both PERMANCOVAs, the random locality factor and the numeric covariable (i.e. depth, in me-ters, and PAR) were significant (Table 3).

Table 3
Results of the different PERMANCOVA designs. Details of the PERMANCOVA tables are available in Supplementary Material V.

	Depth	Par
Random locality factor	P(perm) = 0.0001	P(perm) = 0.001
Numerical covariable	P(perm) = 0.0015	P(perm) = 0.0019
Interaction	P(perm) = 0.0582	P(perm) = 0.0773

Table 2
Results of the different PERMANOVA designs. Details of the PERMANOVA tables are available in Supplementary Material V.

	Depth category	Slope	Orientation	Rugosity
Random locality factor	P(perm) = 0.0001	P(perm) = 0.0001	P(perm) = 0.0001	P(perm) = 0.0003
Fixed environmental factor	P(perm) = 0.2844	P(perm) = 0.7645	P(perm) = 0.7176	P(perm) = 0.7969
Interaction	P(perm) = 0.014	P(perm) = 0.3684	P(perm) = 0.3765	P(perm) = 0.3407

4. Discussion

4.1. The L. stictiforme/cabiochiae species complex encompasses at least eight cryptic species identifiable by barcoding in the French Mediterranean coast

Mitochondrial, plastid and nuclear markers, which belong to different genomes, gave consistent results to reveal distinct haplogroups. In case of asexual reproduction mitochondrial, plastid and nuclear genomes are linked (Dudgeon et al., 2017) thus giving the same information. Inside the C1 species, clonality analyses revealed the absence of duplicated multilocus genotypes. Moreover, the distributions of genetic distances among multilocus genotypes match the distributions obtained with only sexual reproduction (Supplementary Material VIII) suggesting that there are no clones in our dataset. Therefore the consistency of the results obtained with the mitochondrial, plastid and nuclear markers is not likely due to presence of clonal lineages. Those haplogroups were highly divergent for the markers COI and 28S (above 10% of divergence for COI), a level of variation which is generally recognized as interspecific variation for red algae (e.g. Saunders, 2005; Le Gall & Saunders, 2007) and more specifically for coralline algae (e.g. Pardo et al., 2017). In addition, the analyses based on thousands of SNPs confirmed that these seven haplogroups are genetically isolated and highly differentiated even when found in sympatry and even within a single 5 m segment. There is thus no doubt that these haplogroups are reproductively isolated. One may argue that strong inbreeding may create such a pattern (when outcrossing events are rare), and positive F_{IS} values have been reported in other red algae such as *C. crispus* (Kruger-Hadfield et al., 2011 & 2015) and may result from low dispersal capacities leading to inbreeding. Nevertheless, the relatively moderate intra populations F_{IS} values in C1 (Table 4) rule out this hypothesis. We thus established that these haplogroups are separate biological species, i.e. cryptic species of the *Lithophyllum stictiforme/cabiochiae* complex.

Lithophyllum is the most species diverse genus among the Corallinales with 130 species currently recognized (Guiry & Guiry, 2018); however, the use of molecular systematics to clarify relationships among species of the genus *Lithophyllum* highlighted our lack of knowledge on the diversity of this genus (Basso et al., 2015; Hernandez-Kantun et al., 2015 & 2016; Peña et al., 2018). Previous studies (e.g. Bittner et al., 2011; Hernandez-Kantun et al., 2015; Rösler et al., 2016) already underlined the necessity of a detailed molecular study of the *Lithophyllum* genus to unravel potential cryptic diversity. Recently, Pezzolesi et al. (2019) unravelled cryptic diversity in the *L. stictiforme* complex using three barcode markers. Their study showed the presence of at least 13 species at the Mediterranean scale. Our results underline the usefulness of molecular tools to delineate species in this genus, whereas determination of the species *in situ* or by observing classical macro morphological characters is seldom possible.

Table 4
Genetic diversity (expected heterozygosity) and F_{IS} of the C1 species calculated in each population and each locality (in yellow). Populations with a very low individual count (< 9) are colored in grey. *Significant results, ** highly significant results.

Pop	Number of individuals	Gene diversity	F_{IS}
CAS_D1	16	0.1267	0.0245**
CAS_D2	14	0.1226	-0.0096**
CAS	30	0.1249	0.0159**
COU	3	0.1112	-0.2431
FTF_D1	15	0.1172	0.1260**
FTF_D2	15	0.1204	0.0124**
FTF	30	0.1188	0.0696**
LPD	9	0.1090	-0.0477
RMO	3	0.1603	-0.1712

4.2. Community composition and genetic structure cannot wholly be explained by spatial distances and current patterns

At the global scale of this study, the high difference in composition between the Banyuls-sur-mer (westernmost) cryptic species community and all other communities (Fig. 2) is noteworthy. There are three non-exclusive explanations. (1) The scarcity of suitable habitats for these cryptic species (i.e. rocky substratum found in dim light condition) between the Banyuls-sur-mer (BPT) and the Couronne (COU) localities (Martin et al., 2014) may impede the stepwise colonization across these areas, even considering several generations, and the high geographic distance separating Banyuls-sur-mer from the other study sites may impede the colonization in a single generation of propagules (mainly spores in CCA). (2) The Rhône flow at the west of the COU locality and the presence of vortex structures in the Lion Gulf may constitute barriers to dispersal. (3) The different environmental conditions found in Banyuls-sur-mer may select for different cryptic species: salinity and water temperature are highly variable and turbidity is higher in Banyuls-sur-mer compared to any other sampling site (SOMLIT data: http://somlit.epoc.u-bordeaux1.fr/fr/). At the opposite Eastern end of the study, the Villefranche-sur-mer (VPR) community position on the nMDS could be explained both by its eastern geographical origin and by the fact that it was sampled at shallower depth than the other localities (between 15 and 20 m).

Finally, all other localities were clustered on the nMDS (Fig. 2B) in a group gathering the Marseille Area (except the CAS locality), the CIR and the LDM localities, despite the important geographic distances between them. All together this pattern suggests that geographical distance alone does not provide a sufficient explanation of the distribution of these eight cryptic species at the regional scale. Thus, their abundances may be influenced by complicated current patterns and/or by changing environmental factors across the different sampling sites.

At a closer scale around the bay of Marseille, we know the current patterns in more detail and we can benefit from comparative population genetics studies to investigate whether currents and distance can explain species composition (and genetic structure within species). Globally, the *Lithophyllum stictiforme/L. cabiochiae* display a good concordance between cryptic species community and genetic structures in the Marseille Area. The frequencies of the eight cryptic species were highly variable among localities within the Bay of Marseille but three clusters were distinguishable based on community similarities (Fig. 3): (i) the Côte Bleue (COU, CSC, MEJ) and LPD; (ii) Marseille (FTF & RMO), (iii) the PSO and CTF localities. The CAS locality community composition was highly distinct from all the others. The genetic diversity structure within cryptic species C1 presented similarities with the community structure pattern with the same 3 spatial clusters: the CAS population was highly differentiated from all the other populations (Fig. 4 & Supplementary Material VII), the LPD and COU populations on one hand, the FTF and RMO populations on the other hand clustered together on the PCA (Fig. 4A).

Homogenization of species (or allele) frequencies among localities requires both (i) migration of the viable propagules among localities and (ii) successful settlement and growth in new localities (depending among other things on the availability of suitable habitats).

The first condition is mainly determined by the propagules' ability to disperse and the hydrodynamics of water masses in the area (Cowen & Sponaugle, 2009; Weersing & Toonen, 2009). In CCA, propagules have low dispersal capacities and settle closely to their source of emission (Norton, 1992; Opazo & Otaíza, 2007) which can explain the differentiation among localities observed in this study at both the interspecific and the intraspecific levels. Comparing F_{ST} value in this study (F_{ST} global 0.0464) with those obtained by Cahill et al. (2017) using data from several invertebrate species sampled in the same geo-graphic area, the C1 species would correspond to the lecithotroph "larval type" species in terms of dispersal capacities. Both population genomics and cryptic species composition patterns showed a

differentiation between the Côte Bleue, and the east part of the Bay of Marseille. This pattern has been identified in previous studies encompassing 9 animal taxa (Cahill et al., 2017), and a brown alga (Thibaut et al., 2016) and can be attributed to the main currents in the Bay of Marseille that prevent connectivity between these two areas (Pradal & Millet, 2013) at least in sessile organisms with low dispersal abilities (Cahill et al., 2017). The CAS locality presents the highest level of *L. stictiforme/cabiochiae* cryptic species diversity (Table 1) and is also very distinct from the other localities (Fig. 3 B) in species composition. Moreover, within the C1 species, the CAS population is highly differentiated from the others (Fig. 4 & Supplementary Material VII). This sampling locality is east of the head of the "Cassidaigne" marine canyon and presents very different characteristics from other sampled sites, both in terms of currents and biogeochemical parameters. In particular, this locality is not subjected to upwellings as strong as in the area west of the canyon (such as the RMO locality), is more influenced by the North current and often experiences deep eastward currents (Albérola & Millot, 2003; Pairaud et al., 2011).

4.3. Cryptic species community composition is influenced by environmental factors

Indeed, our combined results in community composition and population genomics established that environmental factors are influential in the composition in cryptic species. The cryptic species community in the RMO and CAS localities were different among depth categories. This was especially true in the CAS locality, where the C5 species was totally absent at deepest sites (the D2 depth category) and replaced by the C8 species (Fig. 2). At a higher taxonomic level, Sartoretto et al. (1996) also observed a shift in the frequencies of the main algal builders in coralligenous habitats in the Marseille area across depths: *L. cabiochiae* was reported as the dominant one in deep waters whereas *Mesophyllum alternans* was more restricted to shallower waters. Importantly, no significant genetic differentiation was found for the C1 species between the populations from the D1 and D2 depth categories in the CAS locality (Fig. 4 & Supplementary Material VII), suggesting that gene flow between the two depths is not restricted and propagules can travel between the two depth categories. Thus, the differentiation of the communities between depths (found in the PERMANOVA) should be explained by environmental factors varying across depths such as light or temperature. Light is known to have an influence on cor-alligenous assemblages (Ballesteros, 2006), because CCA only develop at specific values of irradiance (Ballesteros, 1992). Our study shows an influence of the PAR on the community composition of the cryptic species. It could therefore be interesting to experimentally compare physiological parameters of the distinct cryptic species such as photo-synthesis, growth rate, and carbonate precipitation under different level of irradiances. Differences in temperature (particularly in temperature variability) may also have a role but our depth categories (30 m and 40–45 m) are not very contrasted in relation to temperature, both being below the summer thermocline threshold (around 16–20 m) (Harmelin, 2004; Haguenauer et al., 2013). Finally, experimental studies showed that the interaction between light and temperature impacted survival in *L. stictiforme* (Rodríguez-Prieto, 2016).

4.4. Ecological consequences and conservation implications of the cryptic diversity for coralligenous habitats

Different engineering species harboring different ecological traits (Badano & Cavieres, 2006; Lamit et al., 2011) or phenotypic variation among individuals of the same species (Whitham et al., 2003) i n fluence the diversity and structure of the associated communities. Since the cryptic species of the *L. stictiforme/cabiochiae* complex are, together with other CCA of the genus *Mesophyllum,* the main engineers of the coralligenous habitats, the distribution of these cryptic engineering species as well as their intraspecific genetic structure potentially have important consequences on the composition of the benthic assemblages found on coralligenous habitats. CCA are also known to influence the settlement of other invertebrates by producing chemical cues inducing the recruitment of larvae in several habitats (e.g. coral reefs and vermetid reefs) (Diaz-Pulido et al., 2010; Spotorno-Oliveira et al., 2015; Quéré & Nugues, 2015; Elmer et al., 2018). To our knowledge, these kinds of interactions between L. *stictiforme/cabiochiae* and invertebrate larvae (e.g. Anthozoa) have not been studied in coralligenous habitats.

Coralligenous habitats are a major marine biodiversity hotspot of the Mediterranean Sea, yet their protection is still pending mainly because there is still a large gap of knowledge about biodiversity and ecological functioning of these habitats (SPA/RAC, 2017).

Engineer species are priority targets for conservation programs because their protection has a large impact in retaining community and ecosystems integrity and functions (Crain and Bertness, 2006). The high structure found both at the species and the genetic diversity levels make these cryptic species particularly vulnerable to local threats such as water pollution or mechanical degradation. Protecting coralligenous habitats (or just evaluating their vulnerability) requires taking into account the geographic distribution of the eight cryptic species along the French Mediterranean coast and at smaller spatial scales. Due to the high *L. stictiforme/cabiochiae* community composition differentiation between the biogeographic regions of Banyuls-sur-mer, Marseille and Villefranche-sur-mer, it is necessary to consider each of these areas as a unique protection unit. In the Marseille area, the CAS locality harbored the highest level of cryptic species diversity and is the only locality where the C5, C7 and C8 species are found; the C4 species is mainly found on Côte Bleue (Fig. 3 and Table 1). Consequently, to have all the cryptic species under protection requires protecting at least the CAS locality and one locality on the Côte Bleue. Our study strongly suggests that these eight cryptic species have different biotope preferences potentially reflecting contrasted physiological abilities. The ocean acidification and warming components of the global change due to human activity are two of the major threats on coralligenous habitats (Ballesteros, 2006). Recent studies by Rodríguez-Prieto (2016) and Martin et al. (2013) showed that the metabolism, reproduction and survival of the *L. stictiforme/cabiochiae* species complex are affected by irradiance levels, temperature and pCO2. However, in these studies species were identified ignoring the presence of cryptic species and thus missing potential differences of responses of the cryptic species to warming and acidification. It emphasizes the need for more investigations to determine if these different species have different capacities to cope with global change.

Finally, genetic diversity and structure are both key pieces of information needed to design efficient species protection policy. This study is the first that gives an insight into the genetic diversity and structure at the genomic level for the bioengineer algae of coralligenous habitats (C1 species): genetic differentiation occurred at a very small spatial scale resulting from small dispersal capacities of propagules and particularities of the currents in the Marseille area (Fig. 4, Supplementary Material VII). Yet neither the genetic structure at a larger geographical scale nor the impact of selective processes potentially shaping the differentiation between populations living in variable environmental conditions are known. Therefore, investigating genetic diversity and structure in these cryptic species can reveal different capacity (different level of genetic diversity for example) of adaptation to global change which should be considered in conservation policy of coralligenous habitats.

Data statement

Sequences generated by Sanger sequencing are available on Genbank (Accession nos MK838413-MK838443 for 28S, nos MK859621-MK859850 for PsbA, nos MK859851-MK859896 for COI). Sequences generated by Illumina MiSeq are available on Genbank (Accession nos MK861167-MK861439 for 28S and nos MK859377-

MK859620 for PsbA). Raw reads from RNA-seq and capture sequencing are available on Genbank BioProject accession nos PRJNA533203 and PRJNA535387 respectively. Raw reads from MiSeq amplicon sequencing are deposited at DataDryad (https://doi.org/10.5061/dryad.dv4mg). Bioinformatics scripts for processing Miseq amplicon sequencing are available in Github (https://github.com/chaby/dana).

Acknowledgments

We are grateful to the Genotoul bioinformatics platform Toulouse Midi-Pyrenees (Bioinfo Genotoul) for providing help, computing and storage resources. This work benefited from equipment and services from the iGenSeq core facility, at ICM (Paris). We thank the Molecular biology service of the IMBE at the Station Marine d'Endoume (A. Haguenauer, C. Rocher, M. Selva), C. Carpentieri (molecular biologist at the Macherey-Nagel company) for helping with DNA purifications, and the Diving Service of the Pytheas Institute for providing samples.

Funding

This work is a contribution to the Labex OT-Med (no. ANR-11-LABX-0061) funded by the French Government 'Investissements d'Avenir' programme of the French National Research Agency (ANR) through the A*MIDEX project (no. ANR-11-IDEX-0001-02).

Samples were obtained thanks to EraNet (SeasEra) CIGESMED—ANR convention no 12-SEAS-0001-01. Financial support was provided by the project DEVOTES (DEVelopment Of innovative Tools for understanding marine biodiversity and assessing good Environmental Status) funded by the European Union under the 7th Framework Programme, 'The Ocean for Tomorrow' Theme (grant agreement no. 308392), http://www.devotes-project.eu.

Author contributions

AC, J-PF, RD and ADJ conceived the study.

ADJ, ZE, RD, AH, AEC, DG, SS, CR and MS produced the data.

ADJ and AC analyzed the data and wrote the paper.

ADJ, AEC, SS, LLG and AC contributed to manuscript editing and revisions.

Appendix A. Supplementary material

Supplementary data to this article can be found online at https://doi.org/10.1016/j.ympev.2019.04.005.

References

Albérola, C., Millot, C., 2003. Circulation in the French mediterranean coastal zone near Marseilles: the influence of wind and the Northern Current. Cont. Shelf Res. 23 (6), 587–610. https://doi.org/10.1016/S0278-4343(03)00002-5.

Altschul, S.F., Gish, W., Miller, W., Myers, E.W., Lipman, D.J., 1990. Basic local alignment search tool. J. Mol. Biol. 215 (3), 403–410.

Athanasiadis, A., 1999. The taxonomic status of *Lithophyllum stictaeforme* (Rhodophyta, Corallinales) and its generic position in light of phylogenetic considerations. Nordic J. Botany 19 (6), 735–745. https://doi.org/10.1111/j.1756-1051.1999.tb00682.x.

Badano, E.I., Cavieres, L.A., 2006. Impacts of ecosystem engineers on community attributes: effects of cushion plants at different elevations of the Chilean Andes. Divers. Distrib. 12 (4), 388–396. https://doi.org/10.1111/j.1366-9516.2006.00248.x.

Bailleul, D., Stoeckel, S., Arnaud-Haond, S., 2016. RClone: a package to identify MultiLocus Clonal Lineages and handle clonal data sets in r. Methods Ecol. Evol. 7 (8), 966–970. https://doi.org/10.1111/2041-210X.12550.

Balata, D., Piazzi, L., Cecchi, E., Cinelli, F., 2005. Variability of Mediterranean coralligenous assemblages subject to local variation in sediment deposition. Marine Environm. Res. 60 (4), 403–421. https://doi.org/10.1016/j.marenvres.2004.12.005.

Balata, D., Piazzi, L., Cinelli, F., 2007. Increase of sedimentation in a subtidal system: effects on the structure and diversity of macroalgal assemblages. J. Exp. Mar. Biol. Ecol. 351 (1–2), 73–82. https://doi.org/10.1016/j.jembe.2007.06.019. Ballesteros,

E., 1992. Els vegetals i la zonació litoral: espècies, comunitats i factors que influeixen en la seva distribució. Institut d'Estudis Catalans.

Ballesteros, E., 2006. Mediterranean coralligenous assemblages: a synthesis of present knowledge. Oceanogr. Mar. Biol. Annu. Rev. 44, 123–195.

Bandelt, H.J., Forster, P., Röhl, A., 1999. Median-joining networks for inferring intraspecific phylogenies. Mol. Biol. Evol. 16 (1), 37–48. https://doi.org/10.1093/oxfordjournals.molbev.a026036.

Basso, D., Caragnano, A., Gal, L. L., & Rodondi, G. (2015). The genus Lithophyllum in the north-western Indian Ocean, with description of L. yemenense sp. nov. , L. socotraense sp. nov. , L. subplicatum comb. et stat. nov. , and the resumed L. affine , L. kaiseri , and L. subreduncum (Rhodophyta, Corallinales). Phytotaxa, 208(3), 183–200. http://org.doi:10.11646/phytotaxa.208.3.1.

Bittner, L., Payri, C.E., Maneveldt, G.W., Couloux, A., Cruaud, C., de Reviers, B., Le Gall, L., 2011. Evolutionary history of the Corallinales (Corallinophycidae, Rhodophyta) inferred from nuclear, plastidial and mitochondrial genomes. Mol. Phylogenet. Evol. 61 (3), 697–713. https://doi.org/10.1016/j.ympev.2011.07.019.

Boudouresque, C.-F., 2004. Marine biodiversity in the mediterranean: status of spicies, populations and communities. Scientific Reports of the Port-Cros National Park 20, 97–146.

Cabau, C., Escudié, F., Djari, A., Guiguen, Y., Bobe, J., Klopp, C., 2017. Compacting and correcting Trinity and Oases RNA-Seq de novo assemblies. PeerJ 5, e2988. https://doi.org/10.7717/peerj.2988.

Cahill, A.E., De Jode, A., Dubois, S., Bouzaza, Z., Aurelle, D., Boissin, E., Chenuil, A., 2017. A multispecies approach reveals hot spots and cold spots of diversity and connectivity in invertebrate species with contrasting dispersal modes. Mol. Ecol. 26, 6563–6577. https://doi.org/10.1111/mec.14389.

Camacho, C., Coulouris, G., Avagyan, V., Ma, N., Papadopoulos, J., Bealer, K., Madden, T.L., 2009. BLAST+: architecture and applications. BMC Bioinf. 10, 421. https://doi.org/10.1186/1471-2105-10-421.

Chenuil A, Cahill AE, Délémontey N, Du Salliant Du Luc E, Fanton A. (in press). Problems and Questions Posed by Cryptic Species. A Framework to Guide Future Studies. In E. Casetta et al. (eds.), From Assessing to Conserving Biodiversity , History, Philosophy and Theory of the Life Sciences 24, Springer Nature Switzerland. https://doi.org/10.1007/978-3-030-10991-2_4.

Clarke, K.R., Gorley, R.N., Somerfield, P.J., Warwick, R.M., 2014. Change in marine communities: an approach to statistical analysis and interpretation, third ed. PRIMER-E, Plymouth, pp. 260.

Clarke, K.R., Gorley, R.N., 2015. PRIMER v7: User Manual/Tutorial. PRIMER-E, Plymouth, pp. 296.

Cowen, R.K., Sponaugle, S., 2009. Larval dispersal and marine population connectivity. Ann. Rev. Marine Sci. 1 (1), 443–466. https://doi.org/10.1146/annurev.marine.010908.163757.

Crain, C.M., Bertness, M.D., 2006. Ecosystem engineering across environmental gradients: implications for conservation and management. Bioscience 56 (3), 211–218. https://doi.org/10.1641/0006-3568(2006) 056[0211:EEAEGI]2.0.CO;2.

Danecek, P., Auton, A., Abecasis, G., Albers, C.A., Banks, E., DePristo, M.A., Durbin, R., 2011. The variant call format and VCFtools. Bioinformatics 27 (15), 2156–2158. https://doi.org/10.1093/bioinformatics/btr330.

Diaz-Pulido, G., Harii, S., McCook, L.J., Hoegh-Guldberg, O., 2010. The impact of benthic algae on the settlement of a reef-building coral. Coral Reefs 29 (1), 203–208. https://doi.org/10.1007/s00338-009-0573-x.

Dudgeon, S., Kübler, J.E., West, J.A., Kamiya, M., Krueger-Hadfield, S.A., 2017. Asexuality and the cryptic species problem. Perspectives Phycol. 4 (1), 47–59. https://doi.org/10.1127/pip/2017/0070.

Elmer, F., Bell, J.J., Gardner, J.P.A., 2018. Coral larvae change their settlement preference for crustose coralline algae dependent on availability of bare space. Coral Reefs 37 (2), 397–407. https://doi.org/10.1007/s00338-018-1665-2.

Gayral, P., Melo-Ferreira, J., Glémin, S., Bierne, N., Carneiro, M., Nabholz, B., Galtier, N., 2013. Reference-free population genomics from next-generation transcriptome data and the vertebrate-invertebrate gap. PLoS Genet. 9 (4), e1003457. https://doi.org/10.1371/journal.pgen.1003457.

Haas, B. J. (2013). Transdecoder v.3.0.0 https://github.com/TransDecoder/TransDecoder/releases/tag/v3.0.0.

Haguenauer, A., Zuberer, F., Ledoux, J.-B., Aurelle, D., 2013. Adaptive abilities of the Mediterranean red coral Corallium rubrum in a heterogeneous and changing environment: from population to functional genetics. J. Exp. Mar. Biol. Ecol. 449, 349–357. https://doi.org/10.1016/j.jembe.2013.10.010.

Hall, T.A., 1999. BioEdit: a user-friendly biological sequence alignment editor and analysis program for Windows 95/98/NT. Nucleic Acids Symp. Ser. 41, 95–98.

Harmelin, J.-G., 2004. Environnement thermique du benthos côtier de l'île de Port-Cros (parc national, France, Méditerranée nord-occidentale) et implications biogéographiques. Scientific Reports of the Port-Cros National Park 20, 173–194.

Harper, J.T., Saunders, G.W., 2001. The application of sequences of the ribosomal cistron to the systematics and classification of the florideophyte red algae (Florideophyceae, Rhodophyta). Cah. Biol. Mar. 42 (1–2), 25–38.

Hauck, F., 1877. Beitrilge zur Kenntniss der adriatischen Algen. V. Oesterr. Bot. Zeitschr. 27, 292–293.

Hernandez-Kantun, J.J., Rindi, F., Adey, W.H., Heesch, S., Peña, V., Le Gall, L., Gabrielson, P.W., 2015. Sequencing type material resolves the identity and distribution of the generitype *Lithophyllum incrustans*, and related European species L. hibernicum and L. bathyporum (Corallinales, Rhodophyta). J. Phycol. 51 (4), 791–807. https://doi.org/10.1111/jpy.12319.

Guiry, M.D., Guiry, G.M., 2018. AlgaeBase. World-wide electronic publication, National University of Ireland, Galway http://www.algaebase.org.

Hernandez-Kantun, J.J., Gabrielson, P., Hughey, J.R., Pezzolesi, L., Rindi, F., Robinson, N.M., Peña, V., Riosmena-Rodiguez, R., Le Gall, L., Adey, W., 2016. Reassessment of branched *Lithophyllum* spp. (Corallinales, Rhodophyta) in the Caribbean Sea with global implications. Phycologia 55 (6), 619–639. https://doi.org/10.2216/16-7.1.

Hong, J.-S., 1980. Etude faunistique d'un fond de concrétionnement de type coralligène soumis à un gradient de pollution en Méditerrannée nord-occidentale (Golf de Fos).

Faculté des Sciences, Aix-Marseille II.
Jombart, T., 2008. adegenet: a R package for the multivariate analysis of genetic markers. Bioinformatics 24 (11), 1403–1405. https://doi.org/10.1093/bioinformatics/btn129.
Jombart, T., Ahmed, I., 2011. adegenet 1.3-1: new tools for the analysis of genome-wide SNP data. Bioinformatics 27 (21), 3070–3071. https://doi.org/10.1093/bioinformatics/btr521.
Jones, C.G., Lawton, J.H., Shachak, M., 1994. Organisms as Ecosystem Engineers. In *Ecosystem Management*. Springer, New York, NY, pp. 130–147.
Kimura, M., 1980. A simple method for estimating evolutionary rates of base substitutions through comparative studies of nucleotide sequences. J. Mol. Evol. 16 (2), 111–120. https://doi.org/10.1007/BF01731581.
Krueger-Hadfield, S.A., Roze, D., Correa, J.A., Destombe, C., Valero, M., 2015. O father where art thou? Paternity analyses in a natural population of the haploid–diploid seaweed *Chondrus crispus*. Heredity 114 (2), 185–194. https://doi.org/10.1038/hdy.2014.82.
Krueger-Hadfield, Stacy A., Collén, J., Daguin-Thiébaut, C., Valero, M., 2011. Genetic population structure and mating system in chondrus crispus (rhodophyta)1: mating system in chondrus crispus. J. Phycol. 47 (3), 440–450. https://doi.org/10.1111/j.1529-8817.2011.00995.x.
Laborel, J., 1961. Le concretionnement algal “coralligène” et son importance géomorphologique en Méditerranée. Recueil Travaux Station Marine d'Endoume 23, 37–60.
Lamit, L.J., Wojtowicz, T., Kovacs, Z., Wooley, S.C., Zinkgraf, M., Whitham, T.G., Gehring, C.A., 2011. Hybridization among foundation tree species influences the structure of associated understory plant communities. Botany 89 (3), 165–174. https://doi.org/10.1139/b11-006.
Laubier, L. (1966). Le coralligène des Albères : monographie biocénotique. (Vol. 137–316). Monaco: Annales de l’Institut océanographique.
Le Gall, L., Saunders, G.W., 2007. A nuclear phylogeny of the Florideophyceae (Rhodophyta) inferred from combined EF2, small subunit and large subunit ribosomal DNA: Establishing the new red algal subclass Corallinophycidae. Mol. Phylogenet. Evol. 43 (3), 1118–1130. https://doi.org/10.1016/j.ympev.2006.11.012.
Li, H. (2013). Aligning sequence reads, clone sequences and assembly contigs with BWA-MEM. ArXiv:1303.3997 [q-Bio]. Retrieved from http://arxiv.org/abs/1303.3997.
Linares, C., Vidal, M., Canals, M., Kersting, D.K., Amblas, D., Aspillaga, E., Ballesteros, E., 2015. Persistent natural acidification drives major distribution shifts in marine benthic ecosystems. Proc. R. Soc. B 282 (1818), 20150587. https://doi.org/10.1098/rspb.2015.0587.
Lombardi, C., Gambi, M.C., Vasapollo, C., Taylor, P., Cocito, S., 2011. Skeletal alterations and polymorphism in a Mediterranean bryozoan at natural CO2 vents. Zoomorphology 130 (2), 135–145. https://doi.org/10.1007/s00435-011-0127-y.
Martin, C.S., Giannoulaki, M., Leo, F.D., Scardi, M., Salomidi, M., Knittweis, L., Fraschetti, S., 2014. Coralligenous and maërl habitats: predictive modelling to identify their spatial distributions across the Mediterranean Sea. Sci. Rep. 4, 5073. https://doi.org/10.1038/srep05073.
Martin, S., Gattuso, J.-P., 2009. Response of Mediterranean coralline algae to ocean acidification and elevated temperature. Glob. Change Biol. 15 (8), 2089–2100. Martin, S., Cohu, S., Vignot, C., Zimmerman, G., Gattuso, J.-P., 2013. One-year experiment on the physiological response of the Mediterranean crustose coralline alga, Lithophyllum cabiochae, to elevated pCO2 and temperature. Ecol. Evol. 3 (3), 676–693. https://doi.org/10.1002/ece3.475.
Norton, T.A., 1992. Dispersal by macroalgae. Brit. Phycol. J. 27 (3), 293–301. https://doi.org/10.1080/00071619200650271.
Opazo, L.F., Otaíza, R.D., 2007. Vertical distribution of spores of blade-forming *Sarcothalia crispata* (Gigartinaceae) and crustose corallines (Corallinaceae) in the water column. Bot. Mar. 50 (2). https://doi.org/10.1515/BOT.2007.011.
Pairaud, I.L., Gatti, J., Bensoussan, N., Verney, R., Garreau, P., 2011. Hydrology and circulation in a coastal area off Marseille: validation of a nested 3D model with observations. J. Mar. Syst. 88 (1), 20–33. https://doi.org/10.1016/j.jmarsys.2011.02.010.
Paoli, C., Montefalcone, M., Morri, C., Vassallo, P., & Bianchi, C. N. (2016). Ecosystem Functions and Services of the Marine Animal Forests. In S. Rossi, L. Bramanti, A. Gori, & C. Orejas Saco del Valle (Eds.), Marine Animal Forests (pp. 1–42). Cham: Springer International Publishing. http://doi.org/10.1007/978-3-319-17001-5_38-1.
Paradis, E., Claude, J., Strimmer, K., 2004. APE: analyses of phylogenetics and evolution in R language. Bioinformatics 20, 289–290.
Pardo, C., Lopez, L., Peña, V., Hernández-Kantún, J., Le Gall, L., Bárbara, I., Barreiro, R., 2014. A multilocus species delimitation reveals a striking number of species of coralline algae forming maerl in the OSPAR maritime area. PLoS ONE 9 (8), e104073.
Pardo, C., Bárbara, I., Barreiro, R., Peña, V., 2017. Insights into species diversity of associated crustose coralline algae (Corallinophycidae, Rhodophyta) with Atlantic European maerl beds using DNA barcoding. Anales Del Jardín Botánico de Madrid 74 (2), 059.
Peña, V., De Clerck, O., Afonso-Carrillo, J., Ballesteros, E., Bárbara, I., Barreiro, R., Le Gall, L., 2015. An integrative systematic approach to species diversity and distribution in the genus Mesophyllum (Corallinales, Rhodophyta) in Atlantic and Mediterranean Europe. Eur. J. Phycol. 50 (1), 20–36.
Peña, V., Hernandez-Kantun, J.J., Adey, W.H., Gall, L.L., 2018. Assessment of coralline species diversity in the European coasts supported by sequencing of type material: the case study of *Lithophyllum nitorum* (Corallinales, Rhodophyta). Cryptogamie, Algologie 39 (1), 123–137. https://doi.org/10.7872/crya/v39.iss1.2018.123.
Pezzolesi, L., Peña, V., Gall, L.L., Gabrielson, P.W., Kaleb, S., Hughey, J.R., Rindi, F., 2019. Mediterranean Lithophyllum stictiforme (Corallinales, Rhodophyta) is a genetically diverse species complex: implications for species circumscription, biogeography and conservation of coralligenous habitats. J. Phycol. https://doi.org/10.1111/jpy.12837.
Pradal, M.-A., Millet, B., 2013. Spatial heterogeneity of artificial reefs functioning according to wind-induced lagrangian circulation. ISRN Oceanogr. 2013, 1–9. https://doi.org/10.5402/2013/568487.
Quéré, G., Nugues, M.M., 2015. Coralline algae disease reduces survival and settlement success of coral planulae in laboratory experiments. Coral Reefs 34 (3), 863–870. https://doi.org/10.1007/s00338-015-1292-0.
Revell, L.J., 2012. Phytools: an R package for phylogenetic comparative biology (and other things). Methods Ecol. Evol. 3, 217–223. https://doi.org/10.1111/j.2041-210X.2011.00169.x.
Rindi, F., Peña, V., Le Gall L., Braga J. C., Falace A., Hernandez-Kantun, J. J., Pezzolesi, L., Kaleb S. (2017). Evolutionary history and diversity of Mediterranean coralline algae: how much do we know?
Core Team, R., 2017. R: A language and environment for statistical computing. R Foundation for Statistical Computing, Vienna, Austria https://www.R-project.org/.
Rodríguez-Prieto, C., 2016. Light and temperature requirements for survival, growth and reproduction of the crustose coralline *Lithophyllum stictaeforme* from the Mediterranean Sea. Bot. Mar. 59 (2–3). https://doi.org/10.1515/bot-2015-0070.
Romero, G.Q., Gonçalves-Souza, T., Vieira, C., Koricheva, J., 2015. Ecosystem engineering effects on species diversity across ecosystems: a meta-analysis: Ecosystem engineering effects across ecosystems. Biol. Rev. 90 (3), 877–890. https://doi.org/10.1111/brv.12138.
Rösler, A., Perfectti, F., Peña, V., Braga, J.C., 2016. Phylogenetic relationships of corallinaceae (Corallinales, Rhodophyta): taxonomic implications for reef-building corallines. J. Phycol. 52 (3), 412–431. https://doi.org/10.1111/jpy.12404.
Rousset, F., 2008. genepop’007: a complete re-implementation of the genepop software for Windows and Linux. Mol. Ecol. Resour. 8 (1), 103–106. https://doi.org/10.1111/j.1471-8286.2007.01931.x.
Sambrook, J., Fritsch, E. F., & Maniatis, T. (1989). Molecular cloning: a laboratory manual. Molecular Cloning: A Laboratory Manual., (Ed. 2). Retrieved from https://www.cabdirect.org/cabdirect/abstract/19901616061.
Sartoretto, S., Verlaque, M., Laborel, J., 1996. Age of settlement and accumulation rate of submarine “coralligène”(- 10 to- 60 m) of the northwestern Mediterranean Sea; relation to Holocene rise in sea level. Mar. Geol. 130 (3–4), 317–331.
Saunders, G.W., 2005. Applying DNA barcoding to red macroalgae: a preliminary appraisal holds promise for future applications. Philos. Trans. Royal Soc. London B: Biolog. Sci. 360 (1462), 1879–1888. https://doi.org/10.1098/rstb.2005.1719. Smit, A. F. A., Hubley, R. & Green, P. RepeatMasker Open-4.0. 2013-2015 <http://www.repeatmasker.org>. unpublished data. Current Version: open-4.0.6 (RMLib: 20160829 & Dfam: 2.0).
SPA/RAC (2017). Action Plan for the Conservation of the Coralligenous and Other Calcareous Bio-concretions in the Mediterranean Sea. UN Environment/MAP Athens. Greece 2017. Retrieved from http://www.rac-spa.org/sites/default/files/action_plans/pa_coral_en.pdf.
Spotorno-Oliveira, P., Figueiredo, M.A.O., Tâmega, F.T.S., 2015. Coralline algae enhance the settlement of the vermetid gastropod *Dendropoma irregulare* (d’Orbigny, 1842) in the southwestern Atlantic. J. Exp. Mar. Biol. Ecol. 471, 137–145. https://doi.org/10.1016/j.jembe.2015.05.021.
Tamura, K., Dudley, J., Nei, M., Kumar, S., 2007. MEGA4: Molecular Evolutionary Genetics Analysis (MEGA) software version 4.0. Mol. Biol. Evol. 24 (8), 1596–1599. https://doi.org/10.1093/molbev/msm092.
Teagle, H., Hawkins, S.J., Moore, P.J., Smale, D.A., 2017. The role of kelp species as biogenic habitat formers in coastal marine ecosystems. J. Exp. Mar. Biol. Ecol. 492, 81–98. https://doi.org/10.1016/j.jembe.2017.01.017.
Thibaut, T., Bottin, L., Aurelle, D., Boudouresque, C.-F., Blanfuné, A., Verlaque, M., Millet, B., 2016. Connectivity of populations of the Seaweed Cystoseira Amentacea within the bay of Marseille (Mediterranean Sea): genetic structure and hydrodynamic connections. Cryptogamie, Algologie 37 (4), 233–255. https://doi.org/10.7872/crya/v37.iss4.2016.233.
Thierry de Ville d’Avray, D., Ami, D., Chenuil, A., David, R., Féral, J.-P., 2019. Application of the ecosystem service concept at a small-scale: the cases of coralligenous habitats in the North-western Mediterranean Sea. Mar. Pollut. Bull. 138, 160–170. https://doi.org/10.1016/j.marpolbul.2018.10.057.
Tsagkogeorga, G., Cahais, V., Galtier, N., 2012. The population genomics of a fast evolver: high levels of diversity, functional constraint, and molecular adaptation in the Tunicate Ciona intestinalis. Genome Biol. Evol. 4 (8), 852–861. https://doi.org/10.1093/gbe/evs054.
Van der Auwera, G. A., Carneiro, M. O., Hartl, C., Poplin, R., del Angel, G., Levy-Moonshine, et al., (2013). From FastQ data to high confidence variant calls: the Genome Analysis Toolkit best practices pipeline. Current Protocols in Bioinformatics/Editoral Board, Andreas D. Baxevanis et Al., 11(1110), 11.10.1-11.10.33. http://doi.org/10.1002/0471250953.bi1110s43.
Walsh, P.S., Metzger, D.A., Higuchi, R., 1991. Chelex 100 as a medium for simple extraction of DNA for PCR-based typing from forensic material. Biotechniques 10 (4), 506–513.
Weersing, K., Toonen, R., 2009. Population genetics, larval dispersal, and connectivity in marine systems. Mar. Ecol. Prog. Ser. 393, 1–12. https://doi.org/10.3354/meps08287.
Whitham, Thomas G., Young, William P., Martinsen, Gregory D., Gehring, Catherine A., Schweitzer, Jennifer A., Shuster, Stephen M., Kuske, Cheryl R., 2003. Community and ecosystem genetics: a consequence of the extended phenotype. Ecology 84 (3), 559–573. https://doi.org/10.1890/0012-9658(2003) 084[0559:CAEGAC]2.0.CO;2.
Yoon, H.S., Hackett, J.D., Bhattacharya, D., 2002. A single origin of the peridinin-and fucoxanthin-containing plastids in dinoflagellates through tertiary endosymbiosis. Proc. Natl. Acad. Sci. 99 (18), 11724–11729.

Appendix I. Sampling information for each locality. Latitudes and longitudes are north and east, respectively.

Table S1 GPS coordinates of sampling localities. N: number of samples

Locality	Latitude	Longitude	N	Year of collection
Banyuls-sur-mer Pointe du Troc -BPT	42.4806	3.1447	25	2014
Cassidaigne – CAS	43.1799	5.5609	67	2013 & 2014
Corse Ile Rousse – CIR*	42.6487	8.9432	69	2014
Couronne – COU	43.3069	5.1417	19	2014
Frioul – FTF	43.2777	5.2895	51	2014
La Ciotat – CTF	43.1700	5.6088	37	2015
Les Lecques pointe de Defens - LPD	43.1284	5.7494	20	2014
Lion de Mer – LDM	43.4067	6.7728	34	2015
Méjean -MEJ	43.3104	5.2433	58	2014 & 2015
Moyade – RMO	43.2004	5.4004	56	2013 & 2015
Planier – PSO	43.1976	5.2289	28	2013 & 2014
Sec de Carry – CSC	43.3115	5.1395	28	2015
Villefranche-sur-mer Pointe de la Rascasse – VPR	43.6885	7.3083	15	2015

*The CIR locality includes 4 sampling sites: IRP, ISN, CIB and IRG (Table below). The coordinates were calculated using the centroid of the four sampling sites that were effectively sampled. The abundances of each site were summed up because of their geographical proximity.

Table S2 GPS coordinates of the Corsica sampling sites. N: number of samples

Locality	Latitude	Longitude	N	Year of collection
Ile Rousse Petit tombant- IRP	42.6500	8.9486	2	2014
Ile Rousse Sec du Naso -ISN	42.6491	8.9479	34	2014
Ile Rousse Bruschettu -CIB	42.6453	8.9296	15	2014
Ile Rousse Grand tombant - IRG	42.6504	8.9467	18	2014

Appendix II. PCR programs, reaction mixes and primers used to amplify the three barcoding markers : *psb*A, LSU and COI

Table S3 PCR programs and mix used to amplify the psbA, 28S and COI (bold characters) markers

Sequencing Technology	PCR Cycles	PCR Reaction MIX
Sanger	5 ' 94° 38x[30"94°C, 30"50°C, 2'72°C] 4'72°C 4'94°C 40x[40"94°C,40"49°C,1'72°C]	1µL of DNA template, 1.20 µL MgCl2 (stock 25mM), 4 µL of 5X GoTaq® Flexi Buffer,3.2 µL of dNTP(1.25mM), 0.16 µl of each primer, 0.1 of Go-Taq Polymerase (5u/µL), 10.18 µL of H20
Illumina MiSeq PE 2x200pb	2'94°C; 14 × [1'94°C,1'58°C to 45°C (-1°C/cycle), 1'72°C] 25 × [30"94°C, 45"58°C, 45"72°C] 3'72°C	2µL of DNA template, 0.6 of MgCl2 (25mM), 2µL of GoTaq® Flexi Buffer,1.6 µL of dNTP(1.25mM), 0.1 of each primer at 50 µM, 0.05 µl of GoTaq-Flexy Polymerase (5u/µL), 3.55 µL of H20

Table S4 Primers used to amplify the psbA, and LSU markers for MiSeq sequencing

Marker	Primer Forward	Primer reverse	Reference
***psb*A**	**Illumina adapter** CTTTCCCTACACGACGCTCTTCCGATCT **Primer (modified from psbA500F)** CTCTGATGGyATGCCtYTAGG	**Illumina adapter** GGAGTTCAGACGTGTGCTCTTCCGATCT **Primer (modified from psbA-R2)** TCA TGC ATW ACT TCC ATA CCT A	Modified from Yoon et al. 2002
LSU	**Illumina adpater** CTTTCCCTACACGACGCTCTTCCGATCT **Primer** CGTGGGTGAGTCGTTCCTAA	**Illumina adapter** GGAGTTCAGACGTGTGCTCTTCCGATCT **Primer** TT GCA GTT CTA GTT TGG AGC A	Designed for this study

Appendix III. DNA extraction from *Lithohyllum* for capture sequencing

Reagents:

A. Cell lysis buffer: 0.5 M Tris, 0.1 M EDTA, pH 8.8. Autoclaved.

B. 20% SDS. Autoclaved.

C. Protein precipitation solution: 5 M ammonium acetate, pH 8.0, autoclaved. Kept at 4°C.

D. Proteinase K (20 mg/ml)

E. Isopropyl alcohol (Isopropanol). Kept at -20°C.

F. TE (Tris EDTA 1X)

Protocol :

DNA extraction

1. Place algal fragments and in a 5-mm stainless steel bead in a 2 mL Safe Lock tube.
2. Add 537 µL of cell lysis buffer (A) in each tube.
3. Close the lid and grind the samples using a Tissue Lyser II® for 1 min at 30 Hz. Repeat once if necessary.
4. Add 63 µL of 20 % SDS (B) and 5 µL of Proteinase K (D).
5. Vortex briefly
6. Incubate on Eppendorf Thermomixer® at 55 °C and 900 rpm for 3 hours.
7. Centrifuge at 4000G for 4 minutes at 4°C
8. Transfer lysate into a 1.5 mL Safe Lock tube and retrieve the bead (it can be washed and reused)
9. Add 400 µL of protein precipitation solution (C). Agitate by hand.
10. Place the tubes horizontally on ice on a rocking shaker for 5 minutes.
11. Centrifuge at 13 000 rpm for 30 minutes at 4°C.
12. Transfer supernatant in a new 1.5 mL Safe Lock tube.
13. Add 600 µL of isopropanol at -20°C (E) and mix by turning the tubes upside down 30 times.
14. Incubate at -20°C overnight (could be up to 2 days)
15. Centrifuge at 13 000 rpm for 30 minutes at 4 °C.
16. Discard the supernatant and keep the white pellet at the bottom of the tube. By pouring gently the supernatant into trash the pellet should stay stick to the tube. Dry the excess by placing the tubes open upside down on a paper towel.
17. Place the tubes upside up with open lid for 5 minutes at room temperature.
18. Add 175 µL of TE (F). Close the lid and place the tubes at 50 °C for 10 minutes to resuspend DNA. Be sure to resuspend the DNA before proceeding with DNA purification.

DNA purification

The following steps are adapted from Macherey Nagel NucleoSpin® Genomic Clean up manual

1. Heat the DE buffer at 70 °C.
2. Add 525 µL od DB buffer into the 175 µL of resuspended DNA.
3. Vortex for 5 seconds
4. Place the NucleoSpin® gDNA Clean-up Column on a collection tube and load the sample on the column.
5. Centrifuge at 11 000 g for30 seconds. Discard the flow-through
6. Add 700 µL of DW buffer to the column. Vortex for 2 seconds.
7. Centrifuge at 11 000 g for 30 seconds. Discard the flow-through
8. Add 700 µL of DW buffer to the column. Vortex for 2 seconds.
9. Centrifuge at 11 000 g for 30 seconds. Discard the flow-through
10. Centrifuge at 11 000 g for 1 minute. Discard the collection tube.
11. Place the column on the DNA storage tube.
12. Add 50 µL of DE buffer (at 70 °C) on the column. Let it rest for 1 minute at room temperature with an open lid.
13. Centrifuge at 11 000 g for 30 seconds.
14. Add 50 µL of DE buffer (at 70 °C) on the column. Let it rest for 1 minute at room temperature with an open lid.
15. Centrifuge at 11 000 g for 30 seconds.
16. Stock DNA at -20°C

Appendix IV. Haplotypes networks for the three barcoding makers: *psb*A, LSU and COI. Kimura distances between the main haplogroups.

The main groups of haplotypes (hereafter haplogroups) obtained for *psb*A were used as a reference for marker comparisons. Haplotypes were colored according to the *psb*A haplogroup of the individual bearing them (using the add-on Network Publisher).

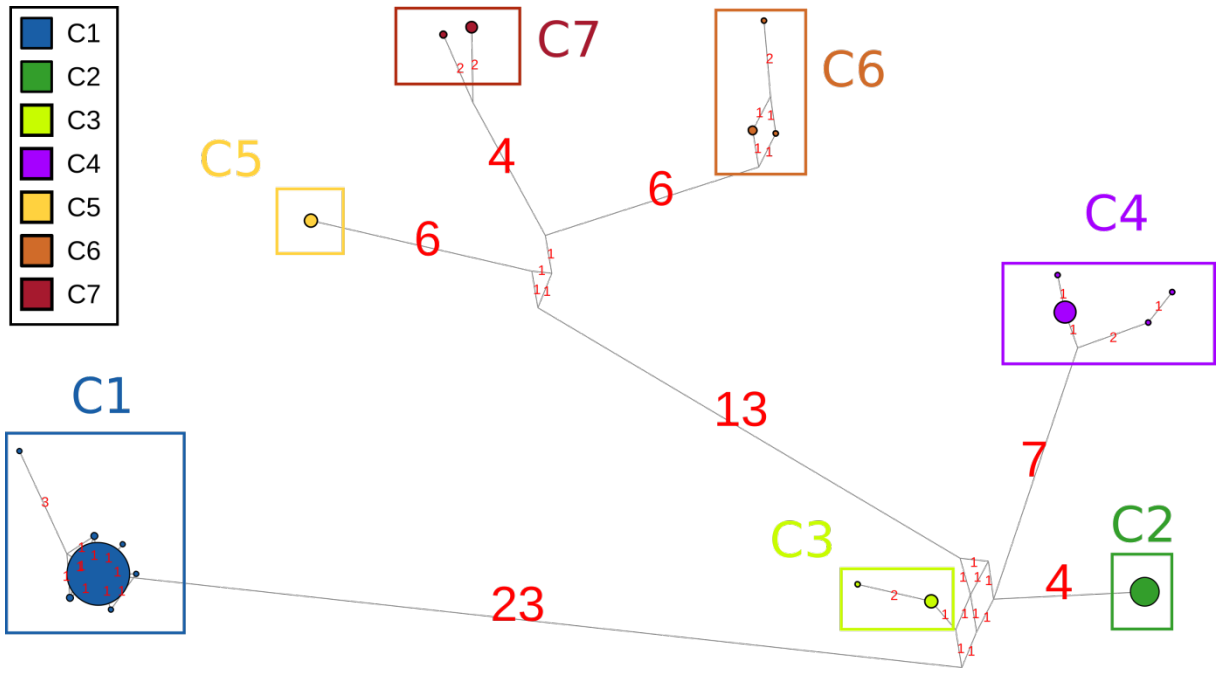

Figure S1 Haplotype network for the psbA marker using 230 sequences (Sanger sequencing) of 744 base pairs

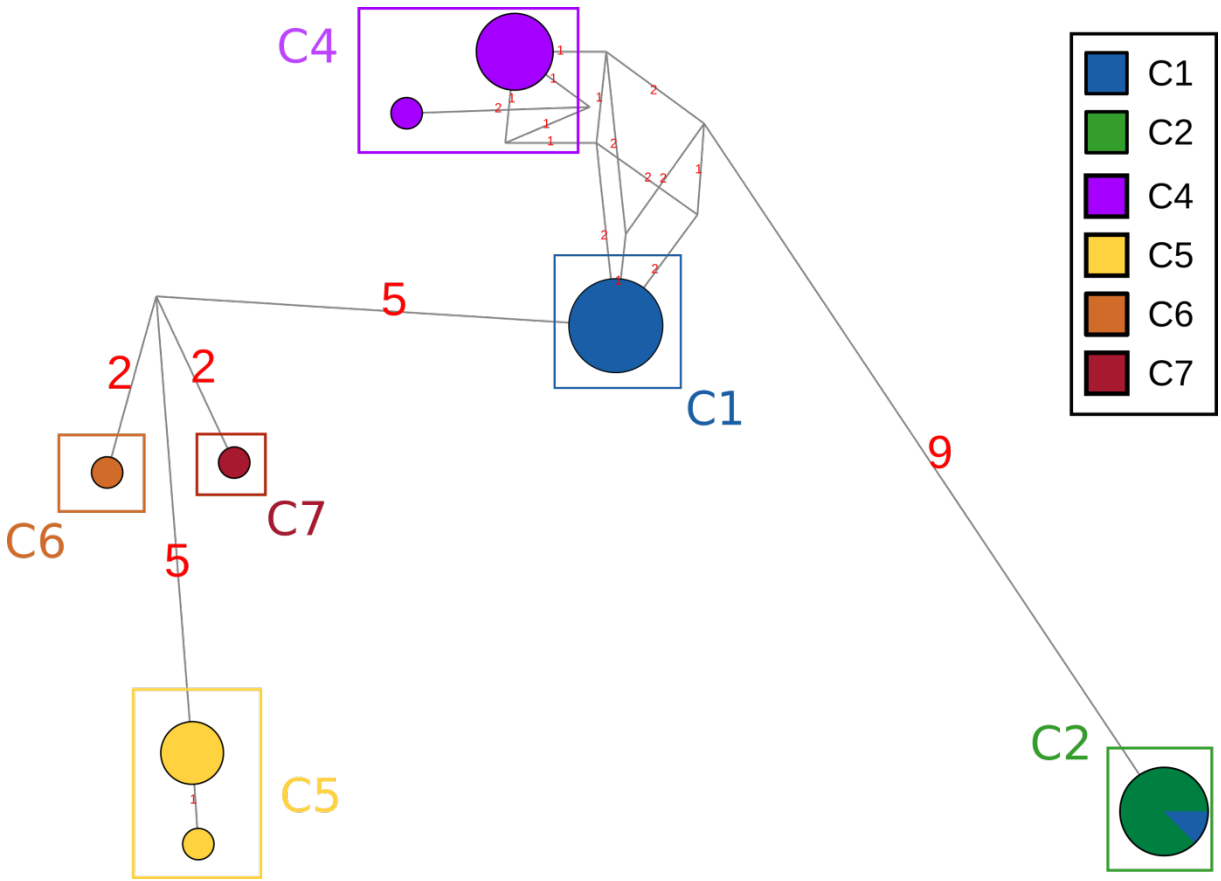

Figure S2 Haplotype network for the 28S marker using 31 sequences (Sanger sequencing) of 802 base pairs

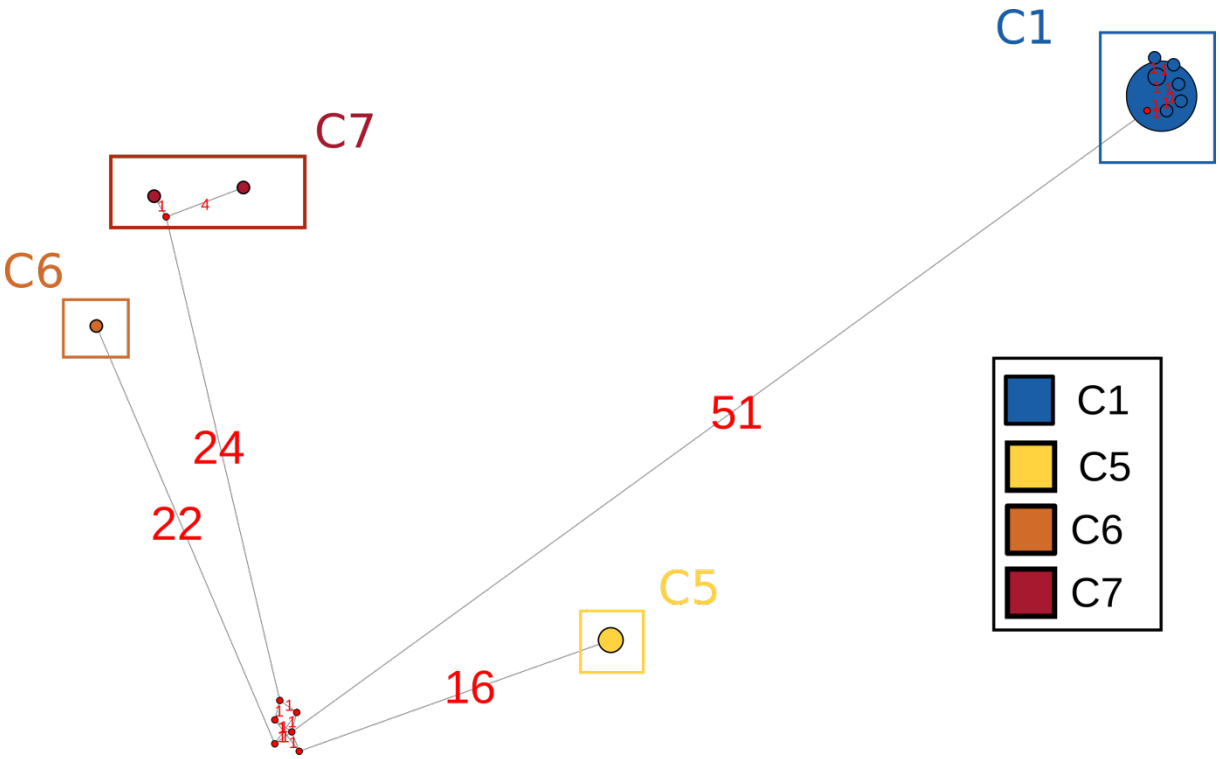

Figure S3 Haplotype network for the COI marker using 46 sequences (Sanger sequencing) of 594 base pairs

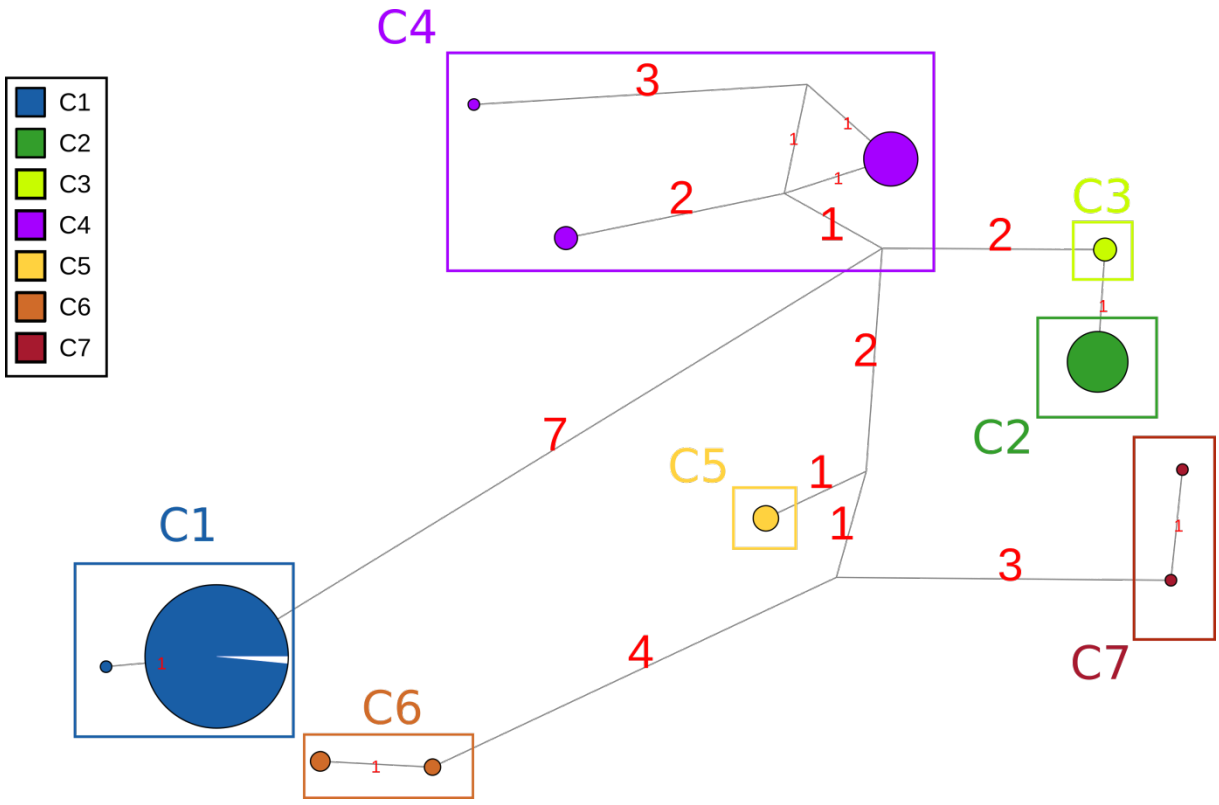

Figure S4 Haplotype network for the psbA marker using 273 sequences (MiSeq sequencing) of 356 base pairs

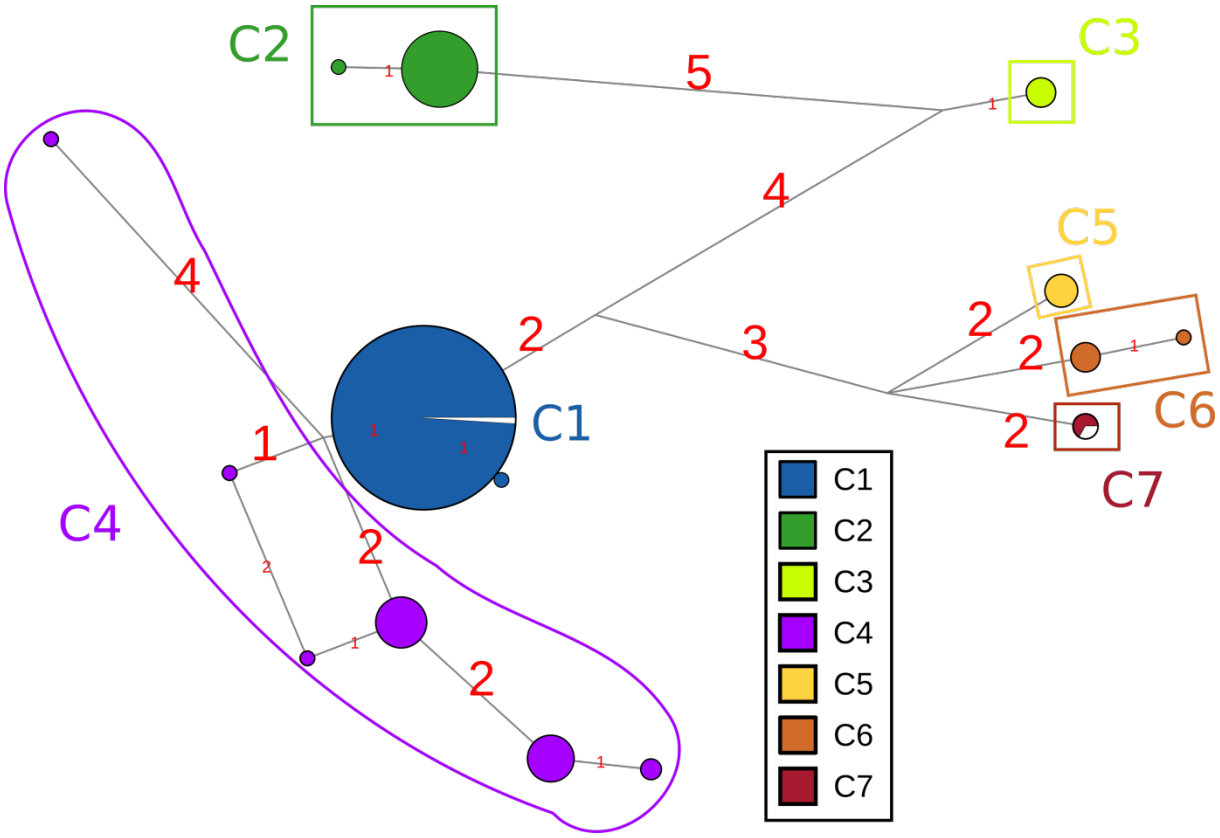

Figure S5 Haplotype network for the 28S marker using 273 sequences (MiSeq sequencing) of 425 base pairs

Table S5 Mean Kimura distances between individuals from the different haplogroups for the psbA marker 744base pairs.

	C1	C2	C3	C4	C5	C6
C2	0.041					
C3	0.035	0.011				
C4	0.038	0.017	0.017			
C5	0.046	0.036	0.032	0.032		
C6	0.053	0.039	0.035	0.037	0.020	
C7	0.053	0.033	0.032	0.034	0.019	0.018

Table S6 Mean Kimura distances between individuals from the same haplogroup for the psbA marker 744 base pairs.

Clade	Intra haplogroup distances
C1	0.0002
C2	0
C3	0.0008
C4	0.001
C5	0
C6	0.002
C7	0.003

Table S7 Mean Kimura distances between individuals from the different haplogroups for the 28S marker 802 base pairs.

	C1	C2	C4	C5	C6
C2	0.013				
C4	0.004	0.017			
C5	0.011	0.018	0.014		
C6	0.007	0.015	0.010	0.005	
C7	0.010	0.018	0.012	0.008	0.003

Table S8 Mean Kimura distances between individuals from the same haplogroup for the 28S marker 802 base pairs. n/c: not calculated

Clade	Intra haplogroup distances
C1	0.003
C2	0
C4	0.0004
C5	0.0006
C6	n/c
C7	n/c

Table S9 Mean Kimura distances between individuals from the different haplogroups for the COI marker 594 base pairs.

	C1	**C5**	**C6**
C5	0.103		
C6	0.105	0.072	
C7	0.104	0.079	0.090

Table S10 Mean Kimura distances between individuals from the same haplogroups for the COI marker base pairs. n/c: not calculated

C1	**0.0008**
C5	0
C6	n/c
C7	0.009

Appendix V. PERMANOVA and PERMANCOVA complete tables for all designs.

Permanova design with Locality as random effect factor and depth category as a fixed effect factor

Resemblance worksheet
Name: Resem4
Data type: Similarity
Selection: All
Standardise Samples by Total
Transform: Square root
Resemblance: S17 Bray-Curtis similarity

Sums of squares type: Type III (partial)
Fixed effects sum to zero for mixed terms
Permutation method: Permutation of residuals under a reduced model
Number of permutations: 9999

Factors

Name	Abbrev.	Type	Levels
LOC	LO	Random	10
Depth	De	Fixed	2

PERMANOVA table of results

Source	df	SS	MS	Pseudo-F	P(perm)	Unique perms	P(MC)
LO	9	48376	5375,1	4,5652	0,0001	9922	0,0001
De	1	4240,6	4240,6	1,2074	0,2844	2990	0,3807
LOxDe**	2	7091,6	3545,8	3,0115	0,014	9958	0,0148
Res	174	2,0487E+05	1177,4				
Total	186	2,7029E+05					

** Term has one or more empty cells

Details of the expected mean squares (EMS) for the model

Source	EMS
LO	1*V(Res) + 17,073*V(LO)
De	1*V(Res) + 14,926*V(LOxDe) + 44,777*S(De)
LOxDe	1*V(Res) + 15,14*V(LOxDe)
Res	1*V(Res)

Construction of Pseudo-F ratio(s) from mean squares

Source	Numerator	Denominator	Num.df	Den.df
LO	1*LO	1*Res	9	174
De	1*De	0,98586*LOxDe + 0,014142*Res	1	2,02
LOxDe	1*LOxDe	1*Res	2	174

Estimates of components of variation

Source	Estimate	Sq.root
V(LO)	245,87	15,68
S(De)	16,266	4,0331
V(LOxDe)	156,43	12,507

V(Res)	1177,4	34,313

Permanova design testing the effect of the depth category factor in the RMO, CAS and FTF localities.

Resemblance worksheet
Name: Resem4
Data type: Similarity
Selection: All
Standardise Samples by Total
Transform: Square root
Resemblance: S17 Bray-Curtis similarity

Sums of squares type: Type III (partial)
Fixed effects sum to zero for mixed terms
Permutation method: Permutation of residuals under a reduced model
Number of permutations: 9999

Factors

Name	Abbrev.	Type	Levels
LOC	LO	Random	10
Depth	De	Fixed	2

PAIR-WISE TESTS

Term 'LOxDe' for pairs of levels of factor 'Depth'

Within level 'CAS' of factor 'LOC'

Groups	t	P(perm)	Unique perms	P(MC)
D2, D1	2,1014	0,0067	8541	0,0076

Denominators

Groups	Denominator	Den.df
D2, D1	1*Res	37

Average Similarity between/within groups

	D2	D1
D2	33,593	
D1	34,375	49,993

Within level 'MOY' of factor 'LOC'

Groups	t	P(perm)	Unique perms	P(MC)
D2, D1	2,1203	0,0573	8	0,0439

Denominators

Groups	Denominator	Den.df
D2, D1	1*Res	28

Average Similarity between/within groups

	D2	D1
D2	100	
D1	84,207	72,102

Within level 'FTF' of factor 'LOC'

Groups	t	P(perm)	Unique perms	P(MC)
D2, D1	1,3056	0,3359	12	0,1936

Denominators

Groups	Denominator	Den.df
D2, D1	1*Res	25

Average Similarity between/within groups

	D2	D1
D2	93,643	
D1	91,045	89,067

Permanova design with locality as random effect factor and slope as a fixed effect factor

Resemblance worksheet
Name: Resem4
Data type: Similarity
Selection: 1-17;19-150;152-187
Standardise Samples by Total
Transform: Square root
Resemblance: S17 Bray-Curtis similarity

Sums of squares type: Type III (partial)
Fixed effects sum to zero for mixed terms
Permutation method: Permutation of residuals under a reduced model
Number of permutations: 9999

Factors

Name	Abbrev.	Type	Levels
LOC	LO	Random	10
Pente	Pe	Fixed	4

PERMANOVA table of results

Source	df	SS	MS	Pseudo-F	P(perm)	Unique perms	P(MC)
LO	9	38278	4253,1	3,4335	0,0002	9895	0,0001
Pe	3	1280	426,66	0,33156	0,7645	9977	0,9391
LOxPe**	8	10693	1336,7	1,0791	0,3684	9936	0,3686
Res	164	2,0315E+05	1238,7				
Total	184	2,6947E+05					

** Term has one or more empty cells

Details of the expected mean squares (EMS) for the model

Source	EMS
LO	1*V(Res) + 12,873*V(LO)
Pe	1*V(Res) + 3,5381*V(LOxPe) + 19,006*S(Pe)

LOxPe	1*V(Res) + 7,1988*V(LOxPe)
Res	1*V(Res)

Construction of Pseudo-F ratio(s) from mean squares

Source	Numerator	Denominator	Num.df	Den.df
LO	1*LO	1*Res	9	164
Pe	1*Pe	0,49149*LOxPe + 0,50851*Res	3	29,38
LOxPe	1*LOxPe	1*Res	8	164

Estimates of components of variation

Source	Estimate	Sq.root
V(LO)	234,17	15,303
S(Pe)	-45,26	-6,7275
V(LOxPe)	13,612	3,6895
V(Res)	1238,7	35,195

Permanova design with locality as random effect factor and orientation as a fixed effect factor

Resemblance worksheet
Name: Resem4
Data type: Similarity
Selection: 1-17;19-75;77-119;121-150;152-187
Standardise Samples by Total
Transform: Square root
Resemblance: S17 Bray-Curtis similarity

Sums of squares type: Type III (partial)
Fixed effects sum to zero for mixed terms
Permutation method: Permutation of residuals under a reduced model
Number of permutations: 9999

Factors

Name	Abbrev.	Type	Levels
LOC	LO	Random	10
Orientation	Or	Fixed	8

PERMANOVA table of results

Source	df	SS	MS	Pseudo-F	P(perm)	Unique perms	P(MC)
LO	9	43219	4802,1	3,9898	0,0001	9925	0,0001
Or	7	6762,8	966,12	0,76861	0,7176	9933	0,7303
LOxOr**	29	36994	1275,7	1,0599	0,3765	9880	0,352
Res	137	1,6489E+05	1203,6				
Total	182	2,6861E+05					

** Term has one or more empty cells

Details of the expected mean squares (EMS) for the model

Source	EMS
LO	1*V(Res) + 11,008*V(LO)

Or	1*V(Res) + 2,185*V(LOxOr) + 11,363*S(Or)
LOxOr	1*V(Res) + 2,9503*V(LOxOr)
Res	1*V(Res)

Construction of Pseudo-F ratio(s) from mean squares

Source	Numerator	Denominator	Num.df	Den.df
LO	1*LO	1*Res	9	137
Or	1*Or	0,74059*LOxOr + 0,25941*Res	7	50,18
LOxOr	1*LOxOr	1*Res	29	137

Estimates of components of variation

Source	Estimate	Sq.root
V(LO)	326,9	18,08
S(Or)	-25,597	-5,0593
V(LOxOr)	24,426	4,9422
V(Res)	1203,6	34,693

Permanova design with locality as random effect factor and rugosity as a fixed effect factor

Resemblance worksheet
Name: Resem4
Data type: Similarity
Selection: 10-13;15;17;19-31;40-97;116-150;152-165;176-187
Standardise Samples by Total
Transform: Square root
Resemblance: S17 Bray-Curtis similarity

Sums of squares type: Type III (partial)
Fixed effects sum to zero for mixed terms
Permutation method: Permutation of residuals under a reduced model
Number of permutations: 9999

Factors

Name	Abbrev.	Type	Levels
LOC	LO	Random	10
Rugosity	Ru	Fixed	4

PERMANOVA table of results

Source	df	SS	MS	Pseudo-F	P(perm)	Unique perms	P(MC)
LO	9	33460	3717,8	3,1936	0,0003	9923	0,0002
Ru	3	1653,1	551,05	0,43177	0,7969	9963	0,8235
LOxRu**	11	14360	1305,5	1,1214	0,3407	9932	0,335
Res	114	1,3271E+05	1164,1				
Total	137	1,8824E+05					

** Term has one or more empty cells

Details of the expected mean squares (EMS) for the model

Source	EMS
LO	1*V(Res) + 9,4821*V(LO)
Ru	1*V(Res) + 3,3034*V(LOxRu) + 16,794*S(Ru)
LOxRu	1*V(Res) + 4,1646*V(LOxRu)
Res	1*V(Res)

Construction of Pseudo-F ratio(s) from mean squares

Source	Numerator	Denominator	Num.df	Den.df
LO	1*LO	1*Res	9	114
Ru	1*Ru	0,79323*LOxRu + 0,20677*Res	3	16,62
LOxRu	1*LOxRu	1*Res	11	114

Estimates of components of variation

Source	Estimate	Sq.root
V(LO)	269,31	16,411
S(Ru)	-43,184	-6,5714
V(LOxRu)	33,946	5,8263
V(Res)	1164,1	34,119

Permanova design with locality as random effect factor and depth category, slope, orientation and rugosity as a fixed effect factors.

Resemblance worksheet
Name: Resem5 pas de données manquantes pour rug
Data type: Similarity
Selection: 1-55;57-81;83-138
Standardise Samples by Total
Transform: Square root
Resemblance: S17 Bray-Curtis similarity

Sums of squares type: Type III (partial)
Fixed effects sum to zero for mixed terms
Permutation method: Permutation of residuals under a reduced model
Number of permutations: 9999

Factors

Name	Abbrev.	Type	Levels
LOC	LO	Random	10
Pente	Pe	Fixed	4
Orientation	Or	Fixed	8
Depth	De	Fixed	1
Rugosity	Ru	Fixed	4

PERMANOVA table of results

Source	df	SS	MS	Pseudo-F	P(perm)	Unique perms	P(MC)
LO	0	0		No test			
Pe	0	0		No test			

Or	0	0		No test			
De	0	0		No test			
Ru	0	0		No test			
LOxPe**	1	594,6	594,6	0,47801	0,6156	9962	0,6342
LOxOr**	3	1845,8	615,26	0,49462	0,75	9960	0,7979
LOxDe	0	0		No test			
LOxRu**	1	636,15	636,15	0,51142	0,5183	9954	0,5897
PexOr**	0	0		No test			
PexDe	0	0		No test			
PexRu**	0	0		No test			
OrxDe	0	0		No test			
OrxRu**	0	0		No test			
DexRu	0	0		No test			
LOxPexOr**	0	0		No test			
LOxPexDe**	0	0		No test			
LOxPexRu**	0	0		No test			
LOxOrxDe**	0	0		No test			
LOxOrxRu**	0	0		No test			
LOxDexRu**	0	0		No test			
PexOrxDe**	0	0		No test			
PexOrxRu**	0	0		No test			
PexDexRu**	0	0		No test			
OrxDexRu**	0	0		No test			
LOxPexOrxDe**	0	0		No test			
LOxPexOrxRu**	0	0		No test			
LOxPexDexRu**	0	0		No test			
LOxOrxDexRu**	0	0		No test			
PexOrxDexRu**	0	0		No test			
LOxPexOrxDexRu**	0	0		No test			
Res	68	84585	1243,9				
Total	135	1,8737E+05					

** Term has one or more empty cells

Details of the expected mean squares (EMS) for the model

Source	EMS
LO	
Pe	
Or	
De	
Ru	
LOxPe	1*V(Res) + 3,6*V(LOxPe)
LOxOr	1*V(Res) + 1,4328*V(LOxOr)
LOxDe	
LOxRu	1*V(Res) + 1,7561*V(LOxRu)
PexOr	
PexDe	
PexRu	
OrxDe	
OrxRu	
DexRu	
LOxPexOr	
LOxPexDe	
LOxPexRu	
LOxOrxDe	

LOxOrxRu	
LOxDexRu	
PexOrxDe	
PexOrxRu	
PexDexRu	
OrxDexRu	
LOxPexOrxDe	
LOxPexOrxRu	
LOxPexDexRu	
LOxOrxDexRu	
PexOrxDexRu	
LOxPexOrxDexRu	
Res	1*V(Res)

Construction of Pseudo-F ratio(s) from mean squares

Source	Numerator	Denominator	Num.df	Den.df
LO			0	0
Pe			0	0
Or			0	0
De			0	0
Ru			0	0
LOxPe	1*LOxPe	1*Res	1	68
LOxOr	1*LOxOr	1*Res	3	68
LOxDe			0	0
LOxRu	1*LOxRu	1*Res	1	68
PexOr			0	0
PexDe			0	0
PexRu			0	0
OrxDe			0	0
OrxRu			0	0
DexRu			0	0
LOxPexOr			0	0
LOxPexDe			0	0
LOxPexRu			0	0
LOxOrxDe			0	0
LOxOrxRu			0	0
LOxDexRu			0	0
PexOrxDe			0	0
PexOrxRu			0	0
PexDexRu			0	0
OrxDexRu			0	0
LOxPexOrxDe			0	0
LOxPexOrxRu			0	0
LOxPexDexRu			0	0
LOxOrxDexRu			0	0
PexOrxDexRu			0	0
LOxPexOrxDexRu			0	0

Estimates of components of variation

Source	Estimate	Sq.root
V(LO)	No test	
S(Pe)	No test	
S(Or)	No test	
S(De)	No test	
S(Ru)	No test	

V(LOxPe)	-180,36	-13,43
V(LOxOr)	-438,75	-20,946
V(LOxDe)	No test	
V(LOxRu)	-346,08	-18,603
S(PexOr)	No test	
S(PexDe)	No test	
S(PexRu)	No test	
S(OrxDe)	No test	
S(OrxRu)	No test	
S(DexRu)	No test	
V(LOxPexOr)	No test	
V(LOxPexDe)	No test	
V(LOxPexRu)	No test	
V(LOxOrxDe)	No test	
V(LOxOrxRu)	No test	
V(LOxDexRu)	No test	
S(PexOrxDe)	No test	
S(PexOrxRu)	No test	
S(PexDexRu)	No test	
S(OrxDexRu)	No test	
V(LOxPexOrxDe)	No test	
V(LOxPexOrxRu)	No test	
V(LOxPexDexRu)	No test	
V(LOxOrxDexRu)	No test	
S(PexOrxDexRu)	No test	
V(LOxPexOrxDexRu)	No test	
V(Res)	1243,9	35,269

Permancova design with locality as random effect factor and depth as a numerical covariable

Resemblance worksheet
Name: Resem5
Data type: Similarity
Selection: 1-17;19-75;77-119;121-150;152-175
Standardise Samples by Total
Transform: Square root
Resemblance: S17 Bray-Curtis similarity

Covariables worksheet
Name: Profondeur Lumière
Data type: Environmental
Sample selection: All
Variable selection: All

Sums of squares type: Type I (sequential)
Fixed effects sum to zero for mixed terms
Permutation method: Permutation of residuals under a reduced model
Number of permutations: 9999

Factors

Name	Abbrev.	Type	Levels
LOC	LO	Random	9

Excluded terms
LUM
lum_2
Depth_lum
LUMxlum_2
LUMxProfondeur
LUMxDepth_lum
LUMxLOC
lum_2xProfondeur
lum_2xDepth_lum
lum_2xLOC
ProfondeurxDepth_lum
Depth_lumxLOC
LUMxlum_2xProfondeur
LUMxlum_2xDepth_lum
LUMxlum_2xLOC
LUMxProfondeurxDepth_lum
LUMxProfondeurxLOC
LUMxDepth_lumxLOC
lum_2xProfondeurxDepth_lum
lum_2xProfondeurxLOC
lum_2xDepth_lumxLOC
ProfondeurxDepth_lumxLOC
LUMxlum_2xProfondeurxDepth_lum
LUMxlum_2xProfondeurxLOC
LUMxlum_2xDepth_lumxLOC
LUMxProfondeurxDepth_lumxLOC
lum_2xProfondeurxDepth_lumxLOC

LUMxlum_2xProfondeurxDepth_lumxLOC

PERMANOVA table of results

Source	df	SS	MS	Pseudo-F	P(perm)	Unique perms
LO	8	51448	6431,1	5,1888	0,0001	9907
Pr	1	7714,9	7714,9	6,2246	0,0015	9957
PrxLO	5	10941	2188,2	1,7655	0,0582	9923
Res	156	1,9335E+05	1239,4			
Total	170	2,6345E+05				

Details of the expected mean squares (EMS) for the model

Source	EMS
LO	1*V(Res) + 18,395*V(LO)
Pr	1*V(Res) + 101,45*S(Pr)
PrxLO	1*V(Res) + 12,572*V(PrxLO)
Res	1*V(Res)

Construction of Pseudo-F ratio(s) from mean squares

Source	Numerator	Denominator	Num.df	Den.df
LO	1*LO	1*Res	8	156
Pr	1*Pr	1*Res	1	156
PrxLO	1*PrxLO	1*Res	5	156

Estimates of components of variation

Source	Estimate	Sq.root
V(LO)	282,23	16,8
S(Pr)	63,831	7,9895
V(PrxLO)	75,469	8,6873
V(Res)	1239,4	35,205

Permancova design with locality as random effect factor and PAR as a numerical covariable

Resemblance worksheet
Name: Resem5
Data type: Similarity
Selection: All
Standardise Samples by Total
Transform: Square root
Resemblance: S17 Bray-Curtis similarity

Covariables worksheet
Name: Profondeur PAR récent
Data type: Environmental
Sample selection: All
Variable selection: All

Sums of squares type: Type I (sequential)

Fixed effects sum to zero for mixed terms
Permutation method: Permutation of residuals under a reduced model
Number of permutations: 9999

Factors

Name	Abbrev.	Type	Levels
LOC	LO	Random	9

Excluded terms
Profondeur
ProfondeurxDepth_lum
ProfondeurxLOC
ProfondeurxDepth_lumxLOC

PERMANOVA table of results

Source	df	SS	MS	Pseudo-F	P(perm)	Unique perms	P(MC)
LO	8	51375	6421,9	5,2286	0,0001	9911	0,0001
De	1	6992,1	6992,1	5,6928	0,0019	9960	0,0033
DexLO	5	10299	2059,7	1,677	0,0773	9933	0,0735
Res	160	1,9652E+05	1228,2				
Total	174	2,6518E+05					

Details of the expected mean squares (EMS) for the model

Source	EMS
LO	1*V(Res) + 18,796*V(LO)
De	1*V(Res) + 94,66*S(De)
DexLO	1*V(Res) + 12,123*V(DexLO)
Res	1*V(Res)

Construction of Pseudo-F ratio(s) from mean squares

Source	Numerator	Denominator	Num.df	Den.df
LO	1*LO	1*Res	8	160
De	1*De	1*Res	1	160
DexLO	1*DexLO	1*Res	5	160

Estimates of components of variation

Source	Estimate	Sq.root
V(LO)	276,32	16,623
S(De)	60,89	7,8032
V(DexLO)	68,586	8,2817
V(Res)	1228,2	35,046

Appendix VI. Mean inter species Euclidean distances.

Table S11 Mean Euclidean distances among haplogroups between individual multilocus genotypes.

	C1	**C2**	**C3**	**C4**	**C5**	**C6**	**C7**	**C8**
C1	16.14							
C2	84.16	20.00						
C3	81.73	59.54	13.19					
C4	80.36	65.76	63.40	24.10				
C5	110.56	115.42	113.95	113.48	22.99			
C6	99.26	104.61	102.88	102.14	64.99	NA		
C7	105.85	111.63	110.08	109.04	71.98	56.11	23.90	
C8	104.15	110.54	108.98	107.73	69.65	53.64	52.76	20.00

Appendix VII. Pairwise F_{ST} between population on the C1 species.

*Table S12 Pairwise population differentiation (F_{ST}). F_{ST} between two depths of the same locality are colored in grey. Populations with low numbers of individuals are colored in red. *Significant results, ** highly significant results*

Pop	CASD1	CASD2	COU	FTFD1	FTFD2	LPD
CASD2	0.0077					
COU	0.0324	0.0468				
FTFD1	0.0551**	0.0656**	0.0296			
FTFD2	0.0533**	0.0599**	0.0229	0.0121		
LPD	0.0500*	0.0591**	0.0626	0.0518*	0.0501	
RMO	0.0691	0.0823	0.0601	0.0452	0.0475	0.0911

Appendix VIII. Frequency distributions of the pairwise alleles differences between MLG in all populations of the C1 species.

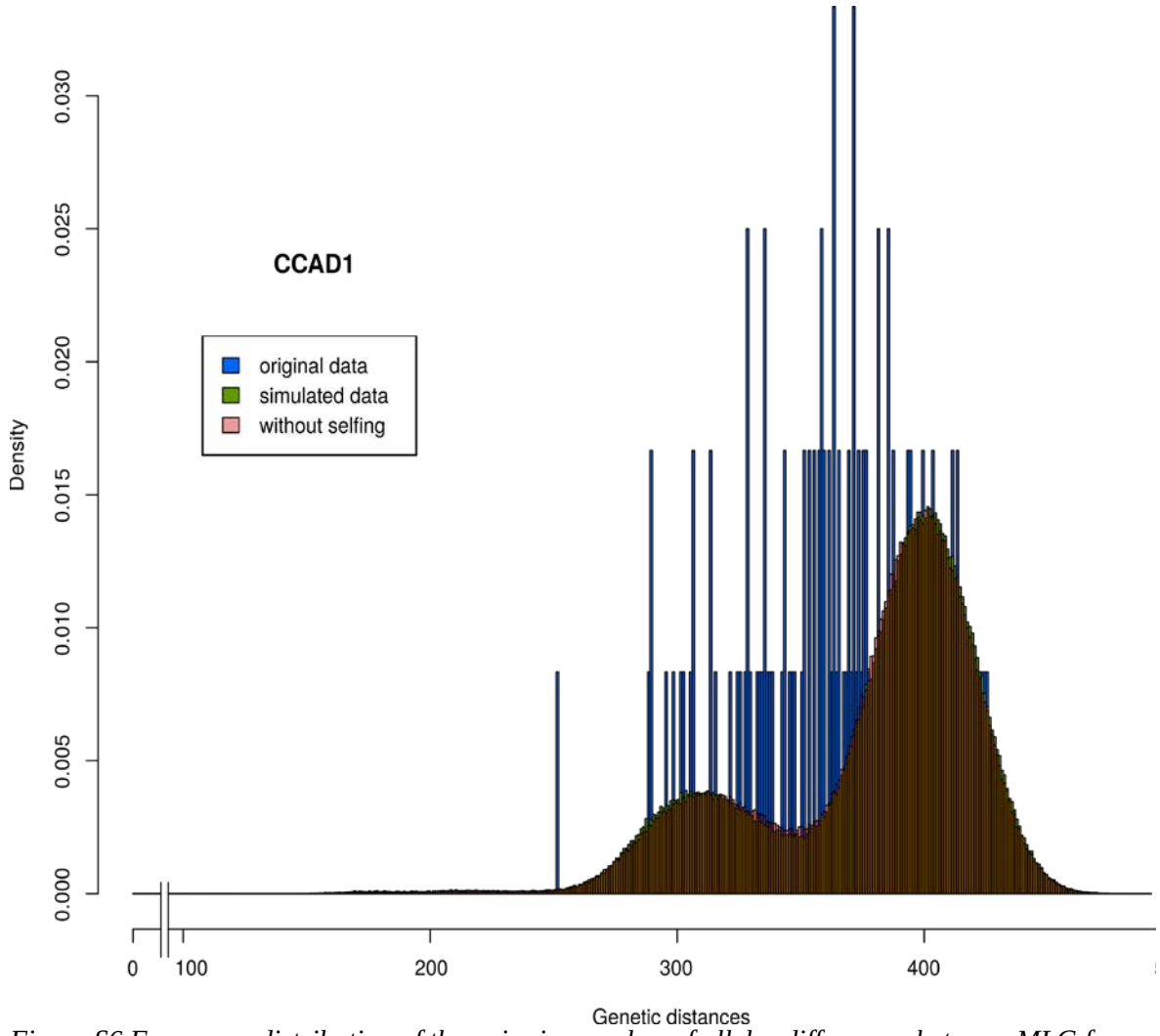

Figure S6 Frequency distribution of the pairwise number of alleles differences between MLG for the CCAD1 population (original data in blue), compared with the frequency of pairwise distances after 1000 sexual events (one generation each, outcrossing and selfing) in which neither identical MLG nor somatic mutations are expected (simulated data in green), and with the frequency distribution of the pairwise distances after 1000 sexual events (one generation each, outcrossing), without selfing (in pink).

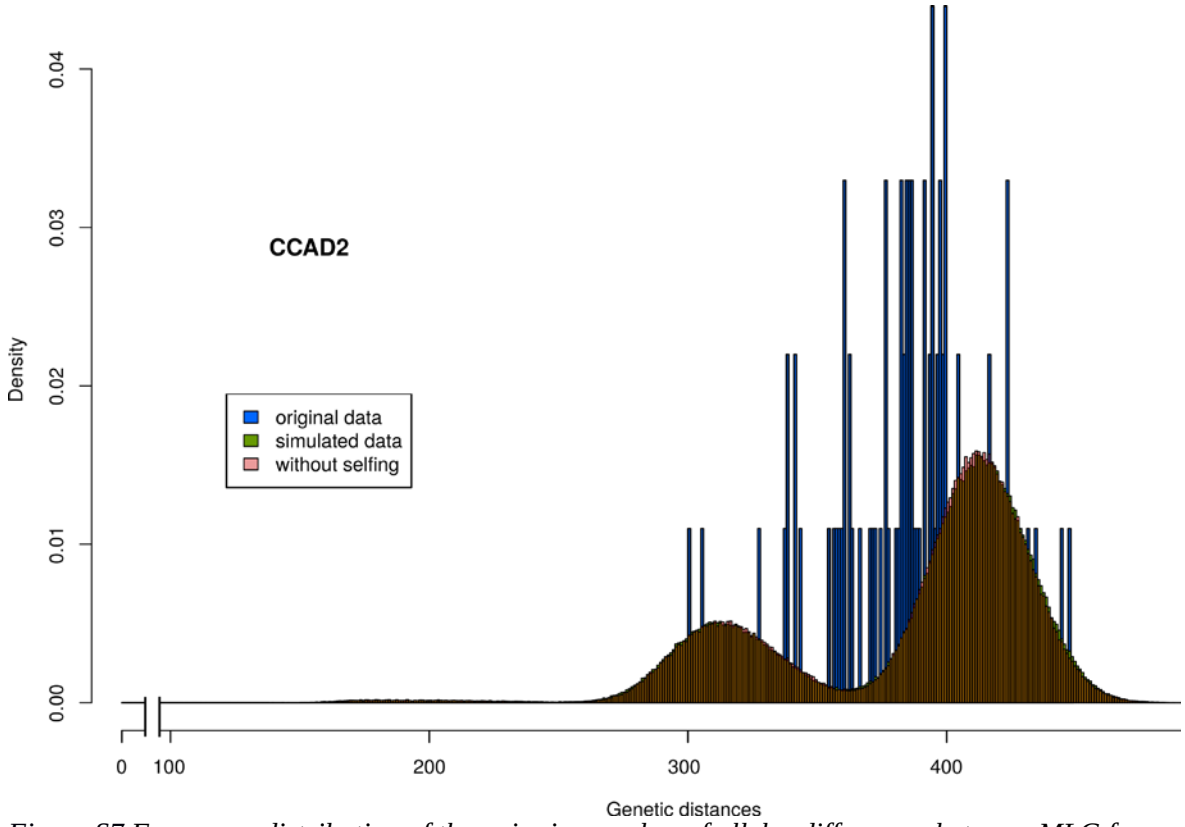

Figure S7 Frequency distribution of the pairwise number of alleles differences between MLG for the CCAD2 population (original data in blue), compared with the frequency of pairwise distances after 1000 sexual events (one generation each, outcrossing and selfing) in which neither identical MLG nor somatic mutations are expected (simulated data in green), and with the frequency distribution of the pairwise distances after 1000 sexual events (one generation each, outcrossing), without selfing (in pink).

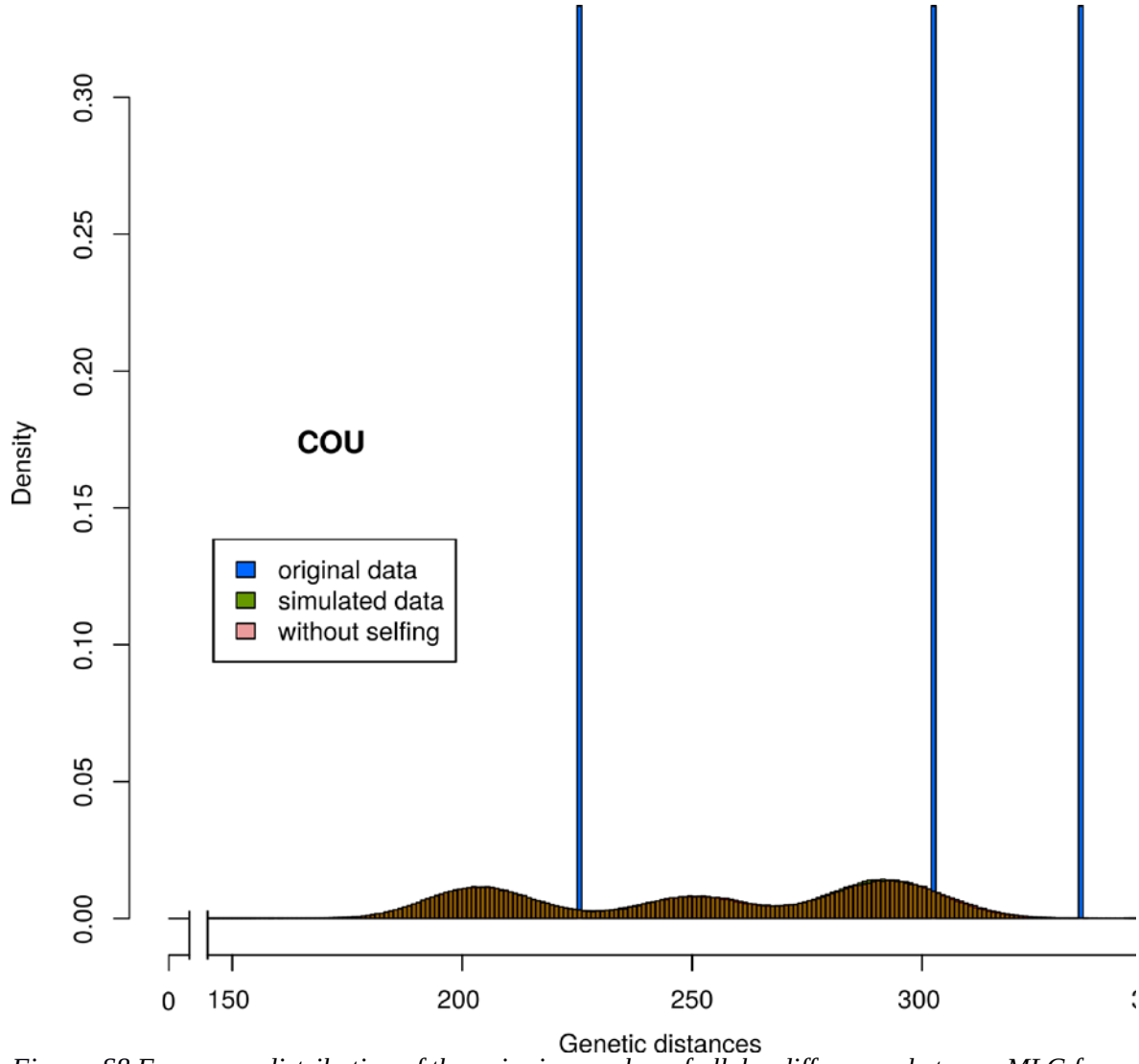

Figure S8 Frequency distribution of the pairwise number of alleles differences between MLG for the COU population (original data in blue), compared with the frequency of pairwise distances after 1000 sexual events (one generation each, outcrossing and selfing) in which neither identical MLG nor somatic mutations are expected (simulated data in green), and with the frequency distribution of the pairwise distances after 1000 sexual events (one generation each, outcrossing), without selfing (in pink).

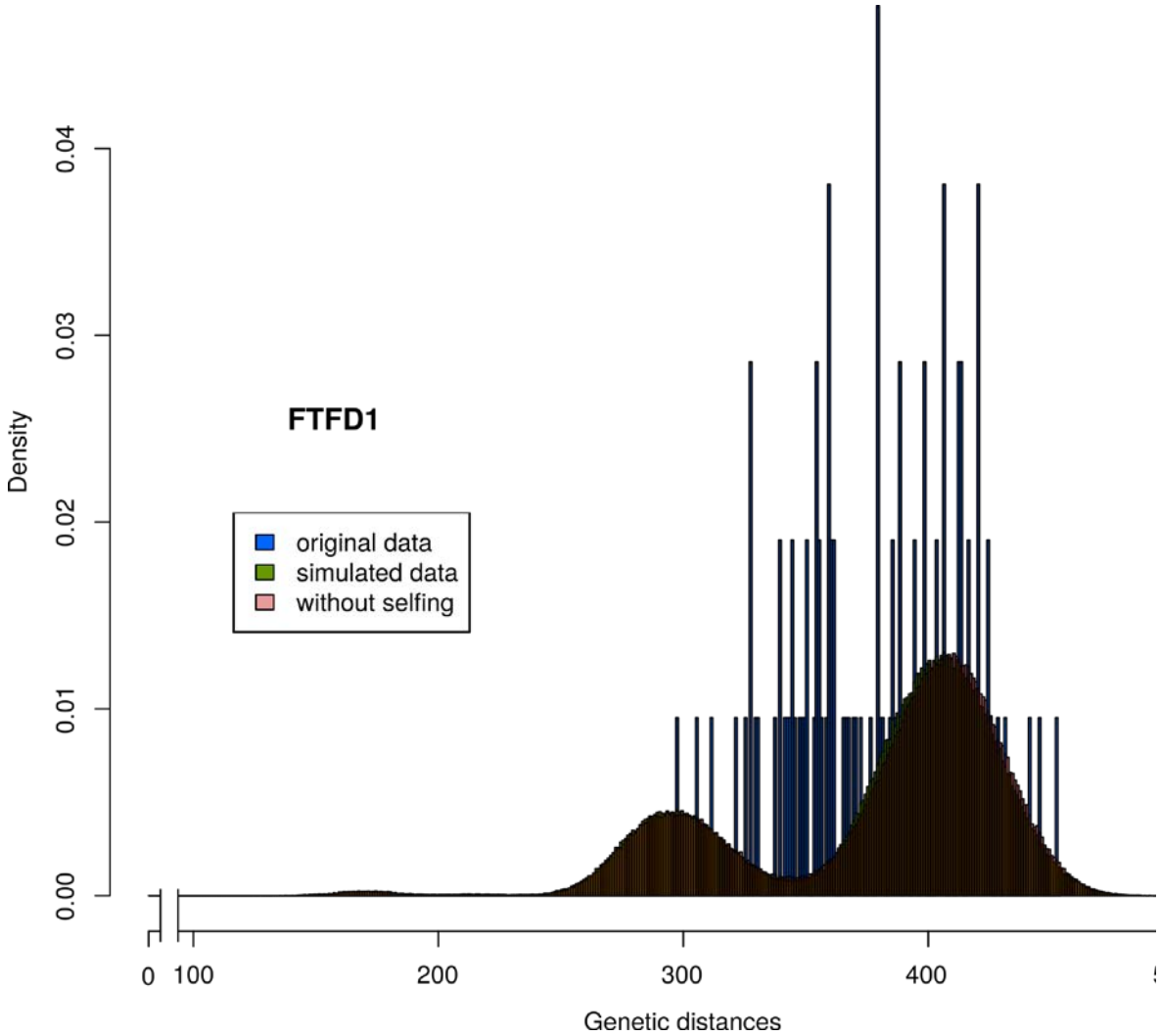

Figure S9 Frequency distribution of the pairwise number of alleles differences between MLG for the FTFD1 population (original data in blue), compared with the frequency of pairwise distances after 1000 sexual events (one generation each, outcrossing and selfing) in which neither identical MLG nor somatic mutations are expected (simulated data in green), and with the frequency distribution of the pairwise distances after 1000 sexual events (one generation each, outcrossing), without selfing (in pink).

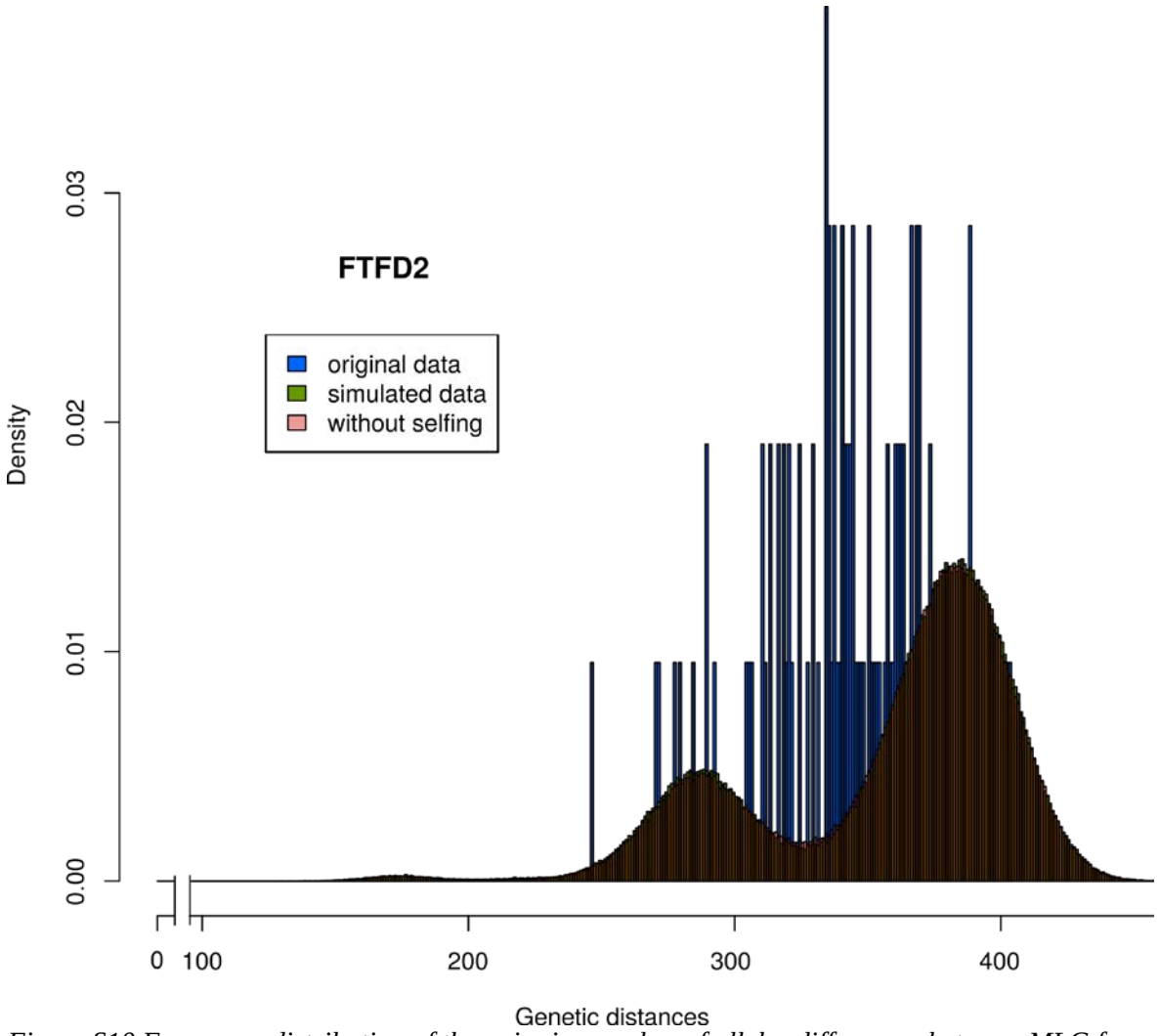

Figure S10 Frequency distribution of the pairwise number of alleles differences between MLG for the FTFD2 population (original data in blue), compared with the frequency of pairwise distances after 1000 sexual events (one generation each, outcrossing and selfing) in which neither identical MLG nor somatic mutations are expected (simulated data in green), and with the frequency distribution of the pairwise distances after 1000 sexual events (one generation each, outcrossing), without selfing (in pink).

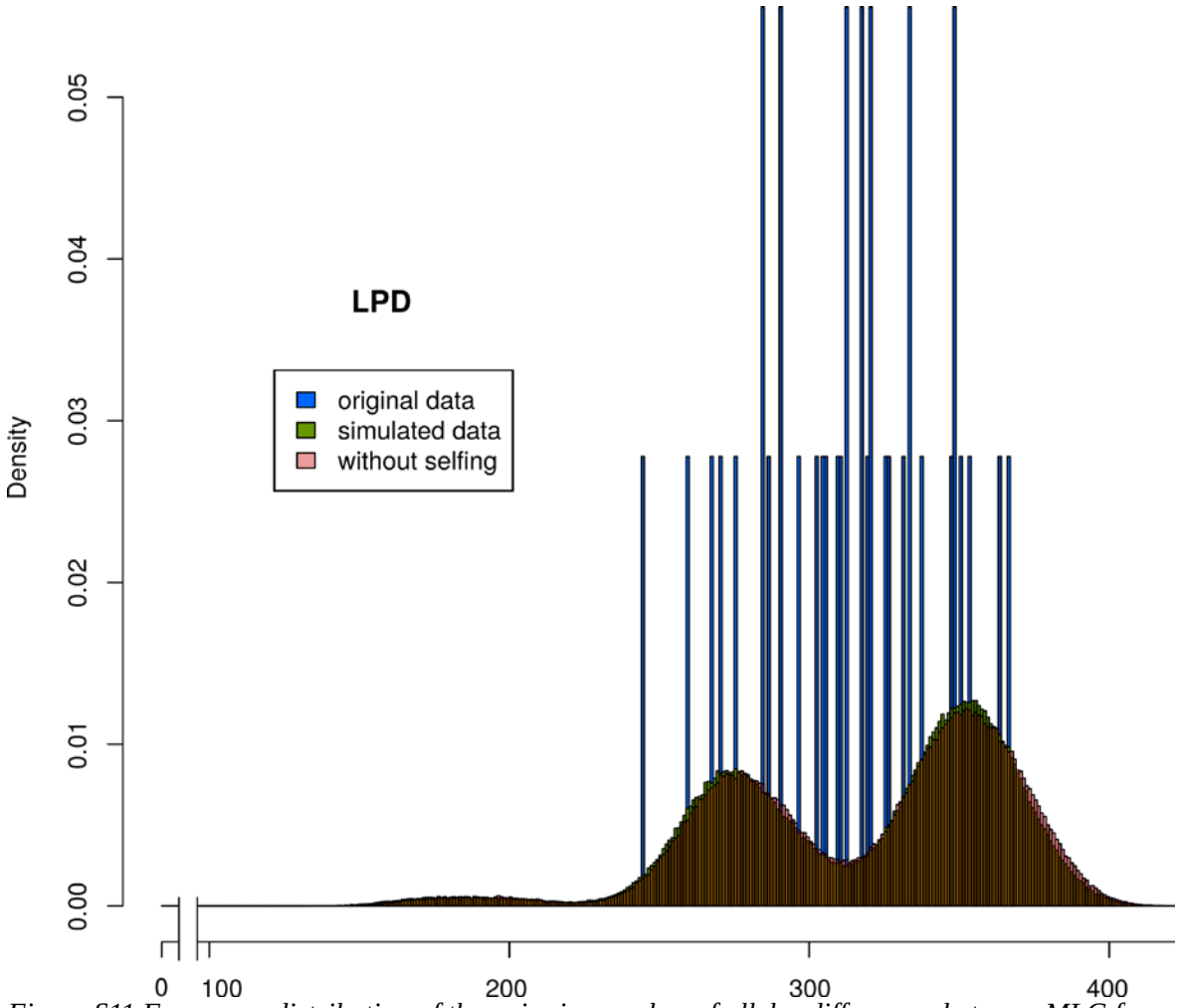

Figure S11 Frequency distribution of the pairwise number of alleles differences between MLG for the LPD population (original data in blue), compared with the frequency of pairwise distances after 1000 sexual events (one generation each, outcrossing and selfing) in which neither identical MLG nor somatic mutations are expected (simulated data in green), and with the frequency distribution of the pairwise distances after 1000 sexual events (one generation each, outcrossing), without selfing (in pink).

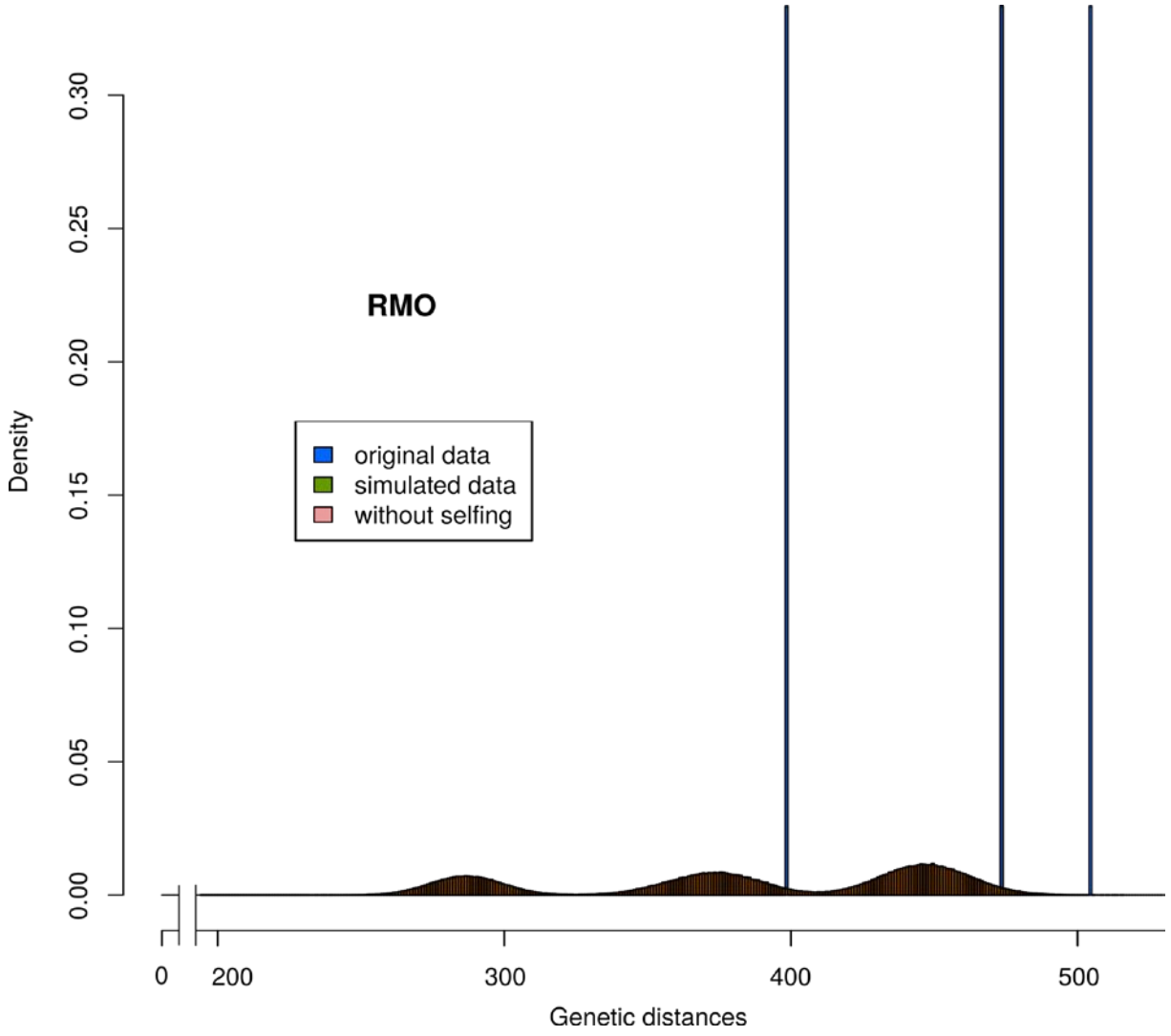

for the RMO population (original data in blue), compared with the frequency of pairwise distances after 1000 sexual events (one generation each, outcrossing and selfing) in which neither identical MLG nor somatic mutations are expected (simulated data in green), and with the frequency distribution of the pairwise distances after 1000 sexual events (one generation each, outcrossing), without selfing (in pink).